Multiple conserved cell adhesion protein interactions mediate neural wiring of a sensory circuit in *C. elegans*

Byunghyuk Kim[1,*] and Scott W. Emmons[1,2,*]

Department of Genetics[1] and Dominick P. Purpura Department of Neuroscience[2], Albert Einstein College of Medicine, Bronx, New York 10461, USA

*Correspondence:

Byunghyuk Kim (byunghyuk.kim@einstein.yu.edu)

Scott W. Emmons (scott.emmons@einstein.yu.edu)

ABSTRACT

Nervous system function relies on precise synaptic connections. A number of widely-conserved cell adhesion proteins are implicated in cell recognition between synaptic partners, but how these proteins act as a group to specify a complex neural network is poorly understood. Taking advantage of known connectivity in *C. elegans*, we identified and studied cell adhesion genes expressed in three interacting neurons in the mating circuits of the adult male. Two interacting pairs of cell surface proteins independently promote fasciculation between sensory neuron HOA and its postsynaptic target interneuron AVG: BAM-2/neurexin-related in HOA binds to CASY-1/calsyntenin in AVG; SAX-7/L1CAM in sensory neuron PHC binds to RIG-6/contactin in AVG. A third, basal pathway results in considerable HOA-AVG fasciculation and synapse formation in the absence of the other two. The features of this multiplexed mechanism help to explain how complex connectivity is encoded and robustly established during nervous system development.

INTRODUCTION

A cardinal feature of the nervous system is its massively large number of specifically connected cells. The effort to reconstruct synaptic connectivity in the nervous system of the nematode *Caenorhabditis elegans* was undertaken in part to study the genetic specification of nervous system structure (Brenner, 1974). One central component of this process must consist of a molecular mechanism during development of synapses for specific cell-cell recognition. Knowledge of the complete connectome places certain requirements and constraints on the possible nature of such a mechanism (Durbin, 1987; Emmons, 2016; Jarrell et al., 2012; White, 1985; White et al., 1983; White et al., 1986). As one example, even in this small (<400 neurons) nervous system, which comprises a sparse neural network, the number of different chemically and electrically coupled cell pairs is large, over 6,000. It is therefore likely that a combinatorial mechanism of some kind is necessary to encode this complexity with a reasonable number of genes.

The mechanism has long been thought to depend on the molecular selectivity of ligand-receptor interactions between cell surface proteins (Sperry, 1963). In *C. elegans*, each neuron connects to multiple (10 or more) other cells — neurons, muscles, and other end organs. Since these sets of target cells intersect, each cell must express multiple such recognition molecules, a different set defining each cell type. The cellular architecture of the nervous system is reproducible, with each neuron process running in a small number of conserved neighborhoods, where it makes *en passant* chemical and gap junction synapses. As a neuron can only synapse onto a cell with which it is in contact, cell recognition events establishing and stabilizing neighborhoods likely play an important role in specifying the connectome (White, 1985; White et al., 1983).

Quantitative analysis showed the strengths of the connections made to different

targets varies continuously over a wide range (Jarrell et al., 2012). This suggests a mechanism that allows for a genetically-specified probability of synapse formation for each pair of cell types. One way to achieve this would be to employ multiple, parallel, pathways acting additively. A multiply over-determined system allows both for robustness and evolvability. It may explain why the overall mechanism remains obscure in spite of decades of forward genetic screens focused on the nervous system and behavior. Multiple additive signals might also account for another feature of the *C. elegans* nervous system, the prevalence of polyadic chemical synapses (69% in hermaphrodites and 66% in males). These might be accounted for if coincident signals from several appropriate postsynaptic target cells increase the probability of presynapse formation. Prior studies in *C. elegans* have implicated interactions with local, albeit non-neuronal, cells in increasing the probability of synapse formation (Colón-Ramos et al., 2007; Shen and Bargmann, 2003).

The *C. elegans* genome contains 106 genes encoding transmembrane or secreted proteins with extracellular protein interaction domains — a structure expected for neural cell-surface recognition molecules (Hobert, 2013). Many of these presumptive cell adhesion genes are conserved in higher animals and their counterparts have been shown to be involved in synapse formation or stabilization (de Wit and Ghosh, 2016).

We initiated our study by determining the expression of this set of 106 genes in the neurons and muscles of the neural network for male mating behavior (in preparation). Based on this expression analysis, here we have analyzed the functions of the cell adhesion genes expressed by a male-specific sensory neuron (HOA) and two of its postsynaptic targets, a sex-shared interneuron (AVG) and a pair of sex-shared sensory neurons (PHCL and PHCR). The neurons make up a part of the circuits for copulatory behavior in the male tail and are necessary for normal male copulatory behavior (Jarrell et al., 2012; Liu and Sternberg, 1995).

We find that the mechanism promoting connectivity of HOA to AVG has precisely the properties proposed above. The neurons express multiple cell adhesion genes. Interactions between a subset of these, two pairs of conserved cell adhesion genes, act together with a basal pathway in three independent pathways that function additively to promote fasciculation of the three neurons, leading to synapse formation.

RESULTS

Two cell adhesion genes, *casy-1* and *rig-6*, are required for patterning of a synaptic vesicle protein and axon fasciculation

For in-depth analysis of circuit formation, we focused on a male-specific circuit that consists of a male-specific sensory neuron, HOA, a sex-shared sensory/interneuron, PHC (a left/right pair of neurons, PHCL and PHCR), and a sex-shared interneuron, AVG (Figure 1A). This circuit has two properties: (1) the axons of the three neurons are highly associated with each other to make a bundle within the male pre-anal ganglion (Figure 1B and C); (2) in this region, the HOA axon forms *en passant* dyadic chemical synapses onto AVG and PHC (Figure 1B and D). (In one animal reconstructed by electron microscopy, there are 44 synapses with AVG and 46 synapses with PHC (Supplementary File 1).) Outside of this region, HOA has many other synaptic targets including male-specific neurons, PVZ, PCA, and some ray sensory neurons (WormWiring: http://wormwiring.org).

AVG, which is mostly postsynaptic to the other neurons, expressed three neural cell adhesion genes in our expression dataset, *casy-1*, *rig-6*, and *sax-3* (Figure 1E). To test whether these genes function for circuit formation, we visualized HOA synaptic output using a fluorescently tagged protein of presynaptic vesicles, mCherry::RAB-3, as a proxy for synaptic connections between HOA and AVG (Figure 1–figure supplement 1) and examined the effects of mutations on the distribution of the presynaptic puncta. We used null mutant alleles, *casy-1(tm718)*, *rig-6(gk438569)* and *sax-3(ky123)*, and a hypomorphic *rig-6(ok1589)* allele, which is predicted to affect three out of four isoforms of RIG-6. (Throughout the paper the hypomorph was used because of its ease of genetics. Its phenotype is the same as the null.) In wild type, multiple RAB-3 puncta were evenly spaced throughout the HOA process (Figure 1F). All mutations disrupted normal puncta distribution: mutants for *casy-1* and *rig-6*

105 often exhibited gaps containing less or smaller puncta, whereas in mutants lacking *sax-3*, the
106 number of RAB-3 puncta was increased due to extra branching of the HOA axon (Figure 1F
107 and G, and Figure 1–figure supplements 2 and 3). SAX-3/Robo is a transmembrane protein
108 with immunoglobulin (Ig) domains and is known to function in axon guidance of multiple
109 types of neurons (Zallen et al., 1999). Thus it is likely that the extra branching phenotype we
110 observed is one of the axon guidance defects in *sax-3* mutants, which we do not pursue
111 further here.

112 GPI-anchored RIG-6/contactin belongs to the Ig superfamily and its loss leads to
113 axon guidance defects of sensory and motorneurons in *C. elegans* (Katidou et al., 2013).
114 CASY-1/calsyntenin is a cadherin domain-containing transmembrane protein. One of its
115 mammalian homologs, calsyntenin-3, has been shown to induce *in vitro* presynapse
116 differentiation when overexpressed postsynaptically (Pettem et al., 2013). As cell contact may
117 be necessary for synapse formation, it was possible that the gap phenotype we observed in
118 *casy-1* and *rig-6* mutants originated from defasciculation of HOA from its target axons. To
119 test this possibility, we examined axon fasciculation between HOA and AVG, along with the
120 HOA presynaptic puncta distribution in the mutants. Indeed, in *casy-1* and *rig-6* mutants, the
121 HOA and AVG axons were frequently detached from each other (Figure 1H and I). Moreover,
122 the axonal segments of HOA detached from AVG had smaller and fewer presynaptic puncta
123 than those contacting AVG (Figure 1H, J and K). This phenotypic association of axon
124 fasciculation and presynaptic pattern was not due to mutational effects, because in wild type
125 animals we also observed, even though rarely, that detached axon segments contained smaller
126 and fewer puncta (Figure 1J and K). Therefore, the HOA presynapse puncta pattern is tightly
127 associated with contacts between HOA and AVG axons, and the gap phenotype we observed
128 in mCherry::RAB-3 labeled presynaptic structures originates most likely from frequent HOA-

AVG defasciculation in mutant animals.

To further examine axon fasciculation among the three associated neurons, HOA, AVG and PHC, in *casy-1* and *rig-6* mutants, we generated transgenic animals whose neurons were labeled with mCherry, TagBFP and GFP, respectively (Figure 2A). We found that the axon fasciculation defects of *casy-1* and *rig-6* mutants were distinguishable from each other: in mutants lacking *casy-1*, the HOA axon was frequently detached from the PHC-AVG axon bundle (Figure 2B and E), whereas in *rig-6* mutants (either *ok1589* or *gk438569*), both HOA and PHC axons were detached from AVG, but the fasciculation of HOA and PHC was not affected (Figure 2C and E, and Figure 2–figure supplement 1). The double mutants of *casy-1* and *rig-6* showed an additive phenotype, in which all three axons were disassociated (Figure 2D and E). Taken together, the results indicate that *casy-1* and *rig-6* are required for proper wiring of the HOA-AVG-PHC circuit, but may function differently to achieve this goal.

Axon fasciculation of HOA and AVG is promoted by PHC

As axon outgrowth and fasciculation are developmental processes, it is possible that the axon fasciculation defects we observed in mutants are affected by developmental timing of axon generation. Therefore we observed axon extension of the three neurons during male development. AVG grows its axon in the embryo and pioneers the right tract of the ventral nerve cord (Durbin, 1987). During the fourth larval stage (L4), in males but not hermaphrodites, PHC extends a process that follows along the axon of AVG (Figure 2F). Later, during the L4-adult transition, HOA extends its axon along the PHC-AVG bundle (Figure 2F). Thus, it is possible that axonal contact between HOA and AVG is promoted by PHC.

To test this possibility, we ablated PHC or HOA and examined axon fasciculation of

153 the remaining neurons. When PHC was ablated, axonal contact between HOA and AVG was
154 compromised, showing a fasciculation defect similar to that observed in *casy-1* and *rig-6*
155 mutants (Figure 2G and H). However, PHC-AVG axonal contact was not affected by HOA
156 ablation (Figure 2G and H). These results suggest there is an affinity between HOA and PHC
157 and raise the possibility that in *rig-6* mutants, the primary defect is loss of adhesion between
158 PHC and AVG, while HOA separates from AVG because of adhesion to PHC.
159
160 **CASY-1 and RIG-6 act in postsynaptic AVG for axon fasciculation**
161 Next, we determined where CASY-1 and RIG-6 act to mediate axon fasciculation. Cell-
162 specific rescue experiments showed that full-length *casy-1* cDNA expressed in postsynaptic
163 AVG, but not presynaptic HOA or PHC, rescued axon fasciculation defects in *casy-1* mutants
164 (Figure 3A). Similarly, only *rig-6* cDNA expression in AVG rescued fasciculation defects of
165 *rig-6* mutants (Figure 3B). These results are consistent with the exclusive expression of *casy-*
166 *1* and *rig-6* genes in AVG as assessed by transcriptional reporters (Figure 1E).
167 The axon bundle and extensive synaptic connections among HOA-AVG-PHC are
168 male-specific and not observed in hermaphrodites (WormWiring: http://wormwiring.org).
169 This raised the possibility that *casy-1* and *rig-6* are male-specifically expressed in AVG to
170 mediate circuit formation. However, we found that transcriptional reporters for these genes
171 are expressed in AVG in both sexes (Figure 3–figure supplement 1). We then examined
172 protein expression in AVG using transgenic animals with YFP-tagged cDNAs. These animals
173 also showed no obvious sex-biased expression (data not shown). In L4 males, right before
174 synapse formation among HOA-AVG-PHC, CASY-1::YFP localized throughout the AVG
175 axon including at potential synaptic sites in the pre-anal ganglion as well as in the anterior
176 cell body (nucleus and cytoplasm) (Figure 3C). YFP::RIG-6 also localized to the axon, but in

the cell body was mainly cytoplasmic (Figure 3D). Taken together, both CASY-1 and RIG-6 function in postsynaptic AVG, possibly by transmembrane adhesion activity of axonally localized proteins, to make an axon fascicle with the presynaptic neurons.

Extracellular domains required for CASY-1 and RIG-6 function

To gain insight into the functional domains and binding partners of CASY-1 and RIG-6, we generated transgenic animals containing a series of deletion constructs for the extracellular domains of the two proteins and tested them for axon fasciculation. CASY-1 contains two cadherin domains and a Laminin, Neurexin, Sex hormone-binding globulin (LNS) domain in its extracellular region (Figure 4A). The full-length (Full) or two cadherin domains-deleted (ΔCads) transgene rescued the fasciculation defect of *casy-1* mutants. However, the LNS domain-deleted (ΔLNS) or all extracellular domains-deleted (ΔNt) transgene failed to rescue the defect (Figure 4A and B). Thus, the LNS domain of CASY-1 is essential for axon fasciculation, but the cadherin domains are dispensable for this function.

RIG-6 has six Ig domains and four fibronectin type III (FN[III]) domains in its extracellular region (Figure 4C). The full-length (Full) or four FN[III] domains-deleted (ΔFN[III]) transgene rescued the fasciculation defect of *rig-6* mutants, whereas Ig domains-deleted (Δ1-3Ig and Δ4-6Ig) transgenes could not (Figure 4C and D), indicating that the Ig domains of RIG-6 are required for axon fasciculation. Taken together, these results suggest that the LNS domain of CASY-1 and the Ig domains of RIG-6 are functionally responsible for axon fasciculation possibly by acting as the binding sites for trans-interacting partners.

Neurexin-related BAM-2 is a presynaptic binding partner of CASY-1

Our finding of HOA-AVG axon defasciculation in *casy-1* mutants (Figure 2) suggests that a presynaptic binding partner may reside in HOA to interact with CASY-1 expressed by AVG. To identify such adhesion factors, we examined mutants for the cell adhesion genes expressed in HOA for defects in HOA presynaptic puncta. Among null mutants for the five genes expressed in HOA in our expression dataset (Figure 1E), *bam-2(cy6)* mutants were identified as showing a gap phenotype similar to the *casy-1* mutant defect (Figure 5A and B, and Figure 5–figure supplement 1).

BAM-2 is a neurexin-related transmembrane protein that regulates axonal branch extension of hermaphrodite-specific VC ventral cord motorneurons in *C. elegans* (Colavita and Tessier-Lavigne, 2003). In a previous study, an interacting partner of a CASY-1 homolog, calsyntenin-3, was shown to be α-neurexin, raising the possibility that BAM-2 is a presynaptic binding partner of CASY-1 (Pettem et al., 2013). Animals lacking *bam-2* showed axon fasciculation defect similar to the phenotype of *casy-1* mutants (Figure 5C and D). Double mutation of *casy-1* and *bam-2* did not enhance the axon fasciculation defect, suggesting that these genes act in the same genetic pathway (Figure 5C and D). Cell-specific rescue showed that full-length *bam-2* cDNA expressed in HOA, but not PHC, rescued axon fasciculation defects in *bam-2* mutants, consistent with the selective expression of *bam-2* in HOA (Figure 5E). Finally, we tested protein interaction of CASY-1 and BAM-2 in a co-immunoprecipitation assay and found that Flag-tagged CASY-1 binds to V5-tagged BAM-2 (Figure 5F). In contrast, NRX-1, a canonical neurexin protein in *C. elegans*, did not bind to CASY-1 (Figure 5–figure supplement 2). These results suggest that BAM-2 is a functional presynaptic binding partner of CASY-1 for axon fasciculation.

A short isoform of SAX-7/L1CAM is a presynaptic binding partner of RIG-6

The *rig-6* mutant axon fasciculation phenotype together with the PHC ablation result (Figure 2) suggest that a binding partner may function in PHC to interact with RIG-6 acting in AVG. Accordingly, we examined HOA presynaptic puncta in null mutants for the five cell adhesion genes expressed in PHC and found *sax-7(nj48)* showed the gap phenotype (Figure 6A and B, and Figure 5–figure supplement 1).

SAX-7/L1CAM, a transmembrane protein with six Ig and five FN[III] domains in its extracellular region, is required in *C. elegans* for maintenance of neuronal position including the cell body and axon (Zallen et al., 1999; Sasakura et al., 2005; Pocock et al., 2008). It has two isoforms – a long form with six Ig domains (SAX-7L) and a short form with four Ig domains (SAX-7S), where SAX-7S is shown to have more adhesive activity for cellular contact (Sasakura et al., 2005; Pocock et al., 2008). Some of the L1 family proteins including L1CAM are known to interact in trans with the RIG-6 ortholog contactin (reviewed in Shimoda and Watanabe, 2009). Several lines of evidence suggest that SAX-7S is a trans-binding partner of RIG-6 for axon fasciculation. First, in *sax-7(nj48)* mutants, the HOA and PHC axons were detached from AVG, but the HOA-PHC fasciculation was intact, which is similar to the phenotype of *rig-6* mutants (Figure 6C and D). Second, the double mutant phenotype of *rig-6;sax-7* animals was similar to that of *rig-6* or *sax-7* single mutants, suggesting that they act genetically in the same pathway (Figure 6C and D). Third, in cell-specific rescue experiments, the short form SAX-7S expressed in PHC, but not in HOA, rescued axon fasciculation defects in *sax-7* mutants, whereas SAX-7L failed to rescue both in PHC and HOA (Figure 6E). This result is also consistent with the selective expression of *sax-7* in PHC (Figure 1E). *sax-7* was expressed in PHC in both sexes (data not shown). Finally, co-immunoprecipitation assay showed that Flag-tagged RIG-6 binds to V5-tagged SAX-7S (Figure 6F).

We observed above that PHC ablation disrupted the HOA-AVG axon fascicle (Figure 2G and H). We asked whether the loss of PHC could be compensated by restoring the interaction of SAX-7S with RIG-6 through expression of SAX-7S in HOA. Indeed, we found that the ectopic expression of SAX-7S in HOA rescued the fasciculation defects caused by PHC ablation (Figure 6G and H). Moreover, a similar rescuing effect was observed in a *casy-1* mutant, but not in a *rig-6* mutant (Figure 6G and H), further supporting the conclusion that SAX-7S binds to RIG-6 and this binding mediates axon fasciculation.

Cell adhesion gene function is required for male behavior

What are the behavioral consequences of the connectivity defects in the circuit described above? The *C. elegans* male displays a stereotyped behavioral sequence during mating: it responds to contact with the hermaphrodite, backs with its tail pressed along the hermaphrodite body, turns at the end to the opposite side, locates its tail at the vulva, and inserts its copulatory spicules for insemination (Liu and Sternberg, 1995). The male-specific HOA sensory neuron is required for the vulva location step of this sequence (Liu and Sternberg, 1995). Recently, it has been found that genetic or laser ablation of AVG or PHC also leads to defects in vulva location (Oren-Suissa et al., 2016; Serrano-Saiz et al., 2017). Thus, we anticipated that the cell adhesion genes required for the HOA-AVG-PHC circuit might affect the vulva location behavior of the male. We examined mating behavior of mutant males for *casy-1*, *rig-6*, *bam-2*, and *sax-7*, and all exhibited vulva location defects (Figure 7A). Double mutants (*casy-1*;*rig-6*, *casy-1*;*bam-2*, and *rig-6;sax-7*) also showed similar behavioral defects (Figure 7A). These defects appear to be specific to the vulva location step, since the male's ability to respond to hermaphrodite contact, the first step of the sequence, was not affected, with the exception of the *sax-7* mutation (Figure 7B). *sax-7* is thought to

mediate multiple aspects of nervous system function including axon guidance, neuronal positioning, and dendrite development (Zallen et al., 1999; Sasakura et al., 2005; Pocock et al., 2008; Dong et al., 2013; Salzberg et al., 2013). In our expression analysis, *sax-7* was also expressed in some of the ray sensory neurons that are known to function in the response step (data not shown), raising the possibility that *sax-7* function in ray neurons is required for the response behavior. Taken together, these results suggest that the cell adhesion proteins described above regulate male mating behavior by mediating the formation of a normally responsive sensory circuit.

DISCUSSION

The specification of HOA > AVG connectivity

We studied requirements for chemical synapse formation between the male-specific sensory neuron HOA and the sex-shared interneuron AVG. We found that three independent pathways promote this connectivity. One involves interactions between cell surface proteins on the processes of HOA and AVG. A second involves another sensory neuron that is also postsynaptic to HOA, PHC, and interactions between cell surface proteins on PHC and AVG. A third pathway we did not identify by itself gives an approximately 50% level of fasciculation and synapse formation between HOA and AVG (Figure 8). Synapse formation between HOA and AVG takes place during the late period of the last, L4, larval stage, when HOA sends out a process along AVG. PHC grows a process fasciculated to AVG before HOA. The role of PHC in promoting HOA fasciculation to AVG is explained by an interaction between HOA and PHC, the molecular basis of which remains to be identified.

The involvement of a third cell such as PHC in promoting synapse formation appears to be a recurring mechanism in *C. elegans*. Epithelial cells of the vulva promote formation of neuromuscular junctions between the HSN motor neuron and vulval muscles (Shen and Bargmann, 2003). The interaction involves binding between Ig-domain cell adhesion molecules SYG-2, expressed by the epithelium, and SYG-1, expressed by HSN (Özkan et al., 2014; Shen et al., 2004). Glial cells promote connection between AIY and RIA interneurons through the UNC-6/netrin pathway (Colón-Ramos et al., 2007). The combined involvement of more than two cells may be a significant way that a combinatorial complexity can be introduced into the mechanism of synaptic specificity.

The features of HOA > AVG connectivity we describe are in remarkable consonance with the features predicted in view of the complexity of the connectome and the structure of

the nervous system. Each cell expresses multiple cell adhesion proteins. A subset of these are involved in formation of one particular synaptic connection. The cell adhesion proteins promote fasciculation, creating an extended neighborhood within which the neurons construct *en passant* synapses. Multiple pathways act independently and additively to create the wild type level of connectivity. We speculate that the pathway that can give rise to a 50% of wild type level of fasciculation even in the absence of the cell adhesion proteins we identified could be the cell lineage itself, which places cells at reproducible locations with reproducible sets of neighbors. As pointed out previously, unless a cell migrates away from its site of birth, it has a limited number of choices for process neighborhoods (White, 1985; White et al., 1983). Involvement of a third cell means lineage specification of that cell also contributes to specifying connectivity.

These features, which help to explain how the complex connectivity can be genetically encoded and robustly established, also explain why, in spite of decades of studies and analysis of thousands of mutations affecting the *C. elegans* nervous system and its behavior, the problem of overall specification of the connectome remains opaque. For connection of HOA to AVG, simultaneous removal of two sets of adhesion protein interactions reduces the level of fasciculation and hence synapse formation by only 50%. It is perhaps telling that some of the earliest uncoordinated mutations identified in *C. elegans*, which define the UNC-6/netrin guidance pathway and do in fact affect connectivity, affect cells that do not run in defined neighborhoods (Brenner, 1973; Hedgecock et al., 1990). Apart from these and some additional effects, in spite of the global role in guidance played by the UNC-6/netrin pathway, in UNC-6/netrin pathway mutants the nervous system remains intact and generally functional. Mutations in other widely-expressed genes for conserved pathways, such as the neurexin/neuroligin interaction and Slit/Robo signaling, have only mild effects on

329 worm behavior. The nervous system is clearly a robust structure that is based on extensive
330 genetic redundancy.

331 We surmounted this obstacle here by taking a candidate gene approach based on a
332 comprehensive expression study. Two similar studies in *C. elegans* based on identifying the
333 expression patterns of Ig-domain transmembrane protein genes followed by examination of
334 mutants found similar axon guidance and fasciculation defects, including additive effects of
335 multiple mutations, similar to the results described here (Aurelio et al., 2002; Schwarz et al.,
336 2009). This approach may be more efficacious than forward genetics for deciphering the
337 genetic code for nervous system connectivity.

338

339 **Synapse formation**

340 For extensively-fasciculated neurons that communicate through *en passant* synapses, the
341 problem of where to locate presynaptic structures must be solved. EM reconstruction shows
342 that in one individual, HOA was fasciculated with AVG over 30 microns. In the fasciculated
343 region 46 presynaptic densities occur in 11 clusters relatively evenly spaced at intervals
344 averaging 1.7 microns (Supplementary File 1). They occur at swellings in the HOA process
345 that contained a mitochondrion. These swellings could be observed with a cytoplasmic
346 marker (Figure 1H). What determines where these swellings, mitochondria, and presynaptic
347 structures are located along the process?

348 We employed a fluorescently tagged protein of presynaptic vesicles, mCherry::RAB-3,
349 to observe presynaptic structures. Absence of mCherry::RAB-3 puncta suggests that
350 components of the presynaptic structure necessary to recruit synaptic vesicles are not
351 assembled at discrete membrane locations. The formation of mCherry::RAB-3 puncta within
352 HOA correlated with apparent fasciculation with AVG and required AVG contact, since in

wild type they were absent or reduced in rare regions of process separation. For recruitment of presynaptic components, the contact signal did not require the cell adhesion genes involved in fasciculation, since in the mutants for these genes, puncta appeared normal in regions of contact (Figure 1). Of the 13 genes we examined, *oig-1* and *oig-8* may be necessary for the formation of puncta, because the mutants lacking them exhibited diffused puncta pattern (Figure 5–figure supplement 1). This diffused puncta phenotype is similar to that of animals lacking SYD-2/Liprin-α, which functions in formation of the presynaptic active zone (Zhen and Jin, 1999), suggesting that *oig-1* and *oig-8* may be involved in organizing presynaptic structures. The identity of the contact signal and how it triggers assembly of presynaptic materials remains elusive.

Functional conservation of cell adhesion protein interactions in synaptic partner recognition

We found that the cell adhesion genes required for promoting fasciculation between HOA and AVG are homologs of genes that have been shown to be involved in axon outgrowth and synapse formation in mammals. A similar finding has been made in wide-ranging prior studies of the *C. elegans* nervous system. Just as so much else of the molecular architecture of the nervous system is conserved across animals, so too, it appears, are the molecular tools that establish synaptic connectivity (Bargmann, 1998). Yet unlike many other aspects of neural function, such as the mechanisms underlying cellular electrical properties or synaptic transmission, connectivity differs profoundly from species to species and accounts for each species' repertoire of behaviors. The resolution of this apparent paradox, of course, is the employment of these generic cell-recognition and adhesion tools with different combinations

in different places. The process is analogous to the specification of diverse cell types by a conserved set of transcription factors.

Our results show that CASY-1/calsyntenin binds to BAM-2/neurexin-related in trans to promote axon-axon adhesion. A similar protein interaction between calsyntenin-3 and α-neurexin has been shown to regulate synapse formation in mammals (Pettem et al., 2013). In addition, through domain analysis of CASY-1, we identified the LNS domain, but not the cadherin domains, is required for axon fasciculation, suggesting that the LNS domain may serve as a binding site for BAM-2 (Figure 4). A biochemical study has shown that the LNS domain of calsyntenin-3 alone is sufficient to bind α-neurexin (Lu et al., 2014). Interestingly, in contrast to CASY-1-BAM-2 interaction, we could not observe protein binding between CASY-1 and NRX-1 (a canonical neurexin in *C. elegans*) in the same experimental condition (Figure 5–figure supplement 2). This suggests that in *C. elegans* BAM-2 may exist as a related but diverged form of neurexin to act as a functional binding partner of CASY-1/calsyntenin. The conserved function of CASY-1/calsyntenin-BAM-2/neurexin-related interaction in neural adhesion and synapse formation seems to be maintained throughout evolution.

Like CASY-1-BAM-2 interaction, protein binding between RIG-6/contactin and SAX-7/L1CAM appears to be molecularly and functionally conserved. A number of protein interactions between contactins (six members: contactin-1-6) and L1 family proteins (four members: L1, CHL1, neurofascin and NrCAM) have been found in vertebrates (Shimoda and Watanabe, 2009; Gennarini et al., 2016). Trans-interactions between these proteins are thought to mediate axon outgrowth via contactin-2 binding to L1 or NrCAM (Kuhn et al., 1991; Stoeckli et al., 1997) and synapse formation via a putative interaction between contactin-5 and NrCAM (Ashrafi et al., 2014). Our domain analysis of RIG-6 indicates that

400 the extracellular Ig domains, but not the FN[III] domains, are required for axon fasciculation,
401 suggesting that RIG-6-SAX-7 interaction might be mediated via the Ig domains (Figure 4).
402 Recent studies have revealed the importance of interactions between Ig domains in cell-cell
403 recognition (Özkan et al., 2013, 2014; Carrillo et al., 2015). Thus, it is possible that the Ig
404 domains of RIG-6 interact directly with the Ig domains of SAX-7 to achieve adhesive
405 function.
406
407 **Implications for neuropsychiatric disorders**
408 There is evidence for each of the four cell adhesion genes described in this study and their
409 related or homologous genes that alterations affecting them are implicated in behavioral
410 deficits or neuropsychiatric disorders. These include: 1) CASY-1/calsyntenin: expression
411 level of calsyntenin-1 or -3 was altered in the human brain or mouse model of Alzheimer's
412 disease (Uchida et al., 2011; Vagnoni et al., 2012). 2) RIG-6/contactin: loss of contactin-4
413 altered axon-target specificity in a visual circuit of mice and relevant behavior (Osterhout et
414 al., 2015); some of contactins (contactin-4-6) are genetically implicated in autism and other
415 mental disorders (Oguro-Ando et al., 2016). 3) BAM-2/neurexin-related: neurexin is a well-
416 known neural adhesion protein involved in autism and other cognitive diseases (Südhof,
417 2008). 4) SAX-7/L1CAM: L1 mutations are associated with diverse neurological defects and
418 mental retardation (Fransen et al., 1997). In our behavioral assays, loss of these adhesion
419 factors disrupted vulva location behavior during male mating (Figure 7). Furthermore, we
420 have shown that these proteins are required for formation of the corresponding sensory circuit.
421 We propose that the cell adhesion proteins may contribute to behavioral performance, in part,
422 through their adhesive functions in circuit assembly.
423

MATERIALS AND METHODS

C. elegans strains, molecular cloning and transgenes

All strains were maintained according to standard methods (Brenner, 1974). *him-5(e1490)* worms were used as reference strains to generate worm populations containing large numbers of males. Worms were grown at 20°C on standard nematode growth media (NGM) plates with OP50 *E. coli* as a food source. Mutant alleles used in this study are *casy-1(tm718) II*, *rig-6(ok1589) II*, *rig-6(gk438569) II*, *sax-3(ky123) X*, *bam-2(cy6) I*, *sax-7(nj48) IV*, *igcm-1(ok711) X*, *nlg-1(ok259) X*, *oig-8(gk867223) II*, *oig-1(ok1687) III*, *lat-1(ok1465) II*, *ncam-1(hd49) X*, *wrk-1(ok695) X*, *zig-1(ok784) II*, *nrx-1(ok1649) V*, *nrx-1(wy778) V*, and *unc-31(e169) IV*.

Information on transgenic strains and DNA constructs used to generate transgenic animals is in Supplementary File 2.

Analysis of electron micrograph

Electron micrograph images of N2Y series for adult male tail were analyzed using Elegance software (Xu et al., 2013). The analyzed sections in this study are from section #13836 (the anterior ends of the PHC axons) to section #14249 (the start point of the anteriorly-oriented HOA axon, which is right after the end point of the PCA axons). For Figure 1B, the image of section #14160 was used. Information on the section numbers, morphology of neurons, synaptic connectivity and images are accessible at WormWiring (http://wormwiring.org).

Microscopy and image analysis

Worms were anesthetized with 10 mM sodium azide and mounted on 5% agar pads on glass slides. We used 1-day-old males unless otherwise indicated. Worms were observed with

448 Nomarski or fluorescence microscopy (Zeiss Axio Imager.A1 or Z2), and images were
449 acquired using the AxioCam camera (Zeiss) and processed using AxioVision (Zeiss). For
450 Figure 3C and D, Z1 Apotome was used to generate z-stacks, and one z-stack image was
451 extracted from them. All figures were prepared using ImageJ software.

452 To measure the number of HOA presynaptic puncta, images were taken with the
453 same amount of exposure time, and the mCherry::RAB-3 puncta that were anterior to the
454 ending of PCA presynaptic signal were counted. The puncta size was measured using a line
455 tool of ImageJ software. To obtain a percentage of axon-axon contact, we summed the
456 lengths of contacting segments divided by total length of the shorter axon. The shorter axons
457 were the HOA axon for HOA-AVG contact, the PHC axons for PHC-AVG contact, and the
458 HOA axon (occasionally PHC) for HOA-PHC contact.

459

460 **Cell ablation**

461 Cell ablation was performed using Pulsed UV, Air-Cooled, Nitrogen Laser System (Spectra-
462 Physics) as described elsewhere (Fang-Yen et al., 2012). The L4-stage males were
463 anesthetized with 10 mM sodium azide and mounted on 5% agar pads on glass slides. Cells
464 were identified with GFP (for PHCs) or wCherry (for HOA) marker. After cell ablations,
465 worms were recovered for 16–24 h and the resulting adult worms were analyzed for imaging.
466 Successful ablations were confirmed under the microscope, otherwise worms were discarded.

467

468 **Co-immunoprecipitation assay**

469 HEK293T cells were cultured in DMEM containing 10% fetal bovine serum, and maintained
470 in 5% CO_2 at 37°C. Plasmids were transfected using Lipofectamine 2000 (Invitrogen)
471 according to manufacturer's instructions. The cells were lysed 24 hours after transfection

with either RIPA lysis buffer (150 mM NaCl, 1% NP-40, 0.5% sodium deoxycholate, 0.1% SDS, 50 mM Tris-HCl [pH 7.4]) or single detergent lysis buffer (150 mM NaCl, 1% NP-40, 50 mM Tris-HCl [pH 8.0]), supplemented with HALT protease inhibitor cocktail (Thermo Scientific). The cell lysates were incubated with mouse monoclonal anti-FLAG M2 (Sigma-Aldrich) for 1 h at 4°C and protein A/G agarose (Santa Cruz Biotechnology) was added to the lysates and then incubated overnight at 4°C. After washed twice with the lysis buffer, the agarose resin was suspended in 1x Laemmli sample buffer (Bio-Rad) and analyzed by immunoblot analysis using anti-FLAG M2 (1:1,000) or mouse monoclonal anti-V5 (1:3,000, Life Technologies).

Male mating behavior assay

Male mating behavior was monitored as described previously (Liu and Sternberg, 1995; Peden and Barr, 2005). L4 males were isolated from hermaphrotides and kept for 16–24 h until they reached adult stage. Mating plates were freshly prepared with a 3µl drop of 10x concentrated OP50 *E.coli* culture, and 10–15 1-day-old *unc-31(e169)* hermaphrodites were placed on the plates. Single adult males were added on the mating plates and analyzed for male behavior. Mating behavior was scored during 5 min or until the male fully stopped at the vulva, whichever occurred first. The numbers of male tail contacts (for response behavior) and passes or hesitations at the vulva (for vulva location behavior) were counted. Successful vulva location was defined as full stop of male tail at the vulva with a duration of 10 sec. Response efficiency is calculated as 1/number of male tail contacts to respond, while vulva location efficiency is calculated as 1/number of encounters to stop (Peden and Barr, 2005).

Statistical analysis

Statistical analysis was performed using GraphPad Prism software (version 7.01). No statistical methods were used to compute sample size when this study was being designed. Statistical methods used are described in each figure legend.

ACKNOWLEDGMENTS

We would like to thank O. Ivashikiv and B. Suo for preparing transcriptional reporter lines; H. Bülow, H. Hutter, S. Mitani, and K. Shen for strains; C. Díaz-Balzac, L. García, Y. Iino, Y. Kohara, and M. Lázaro-Peña for constructs; and H. Bülow and K. Saied-Santiago for their help in conducting co-immunoprecipitation assays. Some strains were provided by the CGC, which is funded by NIH Office of Research Infrastructure Programs (P40 OD010440). Support was from NIH (R01 GM066897 and R01 MH112689) and the G. Harold & Leila Y. Mathers Charitable Foundation.

REFERENCES

Ashrafi, S., Betley, J.N., Comer, J.D., Brenner-Morton, S., Bar, V., Shimoda, Y.,Watanabe, K., Peles, E., Jessell, T.M., and Kaltschmidt, J.A. (2014). Neuronal Ig/Caspr recognition promotes the formation of axoaxonic synapses in mouse spinal cord. Neuron *81*, 120–129.

Aurelio, O., Hall, D.H., and Hobert, O. (2002). Immunoglobulin-domain proteins required for maintenance of ventral nerve cord organization. Science *295*, 686–690.

Bargmann, C.I. (1998). Neurobiology of the Caenorhabditis elegans genome. Science *282*, 2028–2033.

Brenner, S. (1973). The genetics of behaviour. Br. Med. Bull. *29*, 269–271.

Brenner, S. (1974). The genetics of Caenorhabditis elegans. Genetics *77*, 71–94.

Carrillo, R.A., Özkan, E., Menon, K.P., Nagarkar-Jaiswal, S., Lee, P.T., Jeon, M., Birnbaum, M.E., Bellen, H.J., Garcia, K.C., and Zinn, K. (2015). Control of Synaptic Connectivity by a Network of Drosophila IgSF Cell Surface Proteins. Cell *163*, 1770–1782.

Colavita, A., and Tessier-Lavigne M. (2003). A Neurexin-related protein, BAM-2, terminates axonal branches in C. elegans. Science *302*, 293–296.

Colón-Ramos, D.A., Margeta, M.A., and Shen, K. (2007). Glia promote local synaptogenesis through UNC-6 (netrin) signaling in C. elegans. Science *318*, 103–106.

Desbois, M., Cook, S.J., Emmons, S.W., and Bülow, H.E. (2015). Directional Trans-Synaptic Labeling of Specific Neuronal Connections in Live Animals. Genetics *200*, 697–705.

de Wit, J., and Ghosh, A. (2016). Specification of synaptic connectivity by cell surface interactions. Nat. Rev. Neurosci. *17*, 22–35.

Díaz-Balzac, C.A., Lázaro-Peña, M.I., Ramos-Ortiz, G.A., and Bülow, H.E. (2015). The Adhesion Molecule KAL-1/anosmin-1 Regulates Neurite Branching through a SAX-7/L1CAM-EGL-15/FGFR Receptor Complex. Cell Rep. *11*, 1377–1384.

534 Dong, X., Liu, O.W., Howell, A.S., and Shen, K. (2013). An extracellular adhesion molecule
535 complex patterns dendritic branching and morphogenesis. Cell *155*, 296–307.
536 Durbin, R. (1987). Studies on the development and organisation of the nervous system of
537 Caenorhabditis elegans. Ph.D. Thesis, University of Cambridge, Cambridge, England.
538 Emmons, S.W. (2016). Connectomics, the Final Frontier. Curr. Top. Dev. Biol. *116*, 315–330.
539 Fang-Yen, C., Gabel, C.V., Samuel, A.D., Bargmann, C.I., and Avery, L. (2012). Laser
540 microsurgery in Caenorhabditis elegans. Methods Cell. Biol. *107*, 177–206.
541 Fransen, E., Van Camp, G., Vits, L., and Willems, P.J. (1997). L1-associated diseases: clinical
542 geneticists divide, molecular geneticists unite. Hum. Mol. Genet. *6*, 1625–1632.
543 Gennarini, G., Bizzoca, A., Picocci, S., Puzzo, D., Corsi, P., and Furley, A.J. (2016). The role
544 of Gpi-anchored axonal glycoproteins in neural development and neurological disorders.
545 Mol. Cell Neurosci. http://dx.doi.org/10.1016/j.mcn.2016.11.006.
546 Hedgecock, E.M., Culotti, J.G., and Hall, D.H. (1990). The unc-5, unc-6, and unc-40 genes
547 guide circumferential migrations of pioneer axons and mesodermal cells on the epidermis
548 in C. elegans. Neuron *4*, 61–85.
549 Hobert, O. (2002). PCR fusion-based approach to create reporter gene constructs for
550 expression analysis in transgenic *C. elegans*. Biotechniques *32*, 728–730.
551 Hobert, O. (2013). The neuronal genome of Caenorhabditis elegans. WormBook, 1–106. doi:
552 10.1895/wormbook.1.161.1.
553 Hunt-Newbury, R., Viveiros, R., Johnsen, R., Mah, A., Anastas, D., Fang, L., Halfnight, E.,
554 Lee, D., Lin, J., Lorch, A., et al. (2007). High-throughput in vivo analysis of gene
555 expression in Caenorhabditis elegans. PLoS Biol. *5*, e237.
556 Ikeda, D.D., Duan, Y., Matsuki, M., Kunitomo, H., Hutter, H., Hedgecock, E.M., and Iino, Y.
557 (2008). CASY-1, an ortholog of calsyntenins/alcadeins, is essential for learning in

Caenorhabditis elegans. Proc. Natl. Acad. Sci. USA *105*, 5260–5265.

Jarrell, T.A., Wang, Y., Bloniarz, A.E., Brittin, C.A., Xu, M., Thomson, J.N., Albertson, D.G., Hall, D.H., and Emmons, S.W. (2012). The connectome of a decision-making neural network. Science *337*, 437–444.

Katidou, M., Tavernarakis, N., and Karagogeos, D. (2013). The contactin RIG-6 mediates neuronal and non-neuronal cell migration in Caenorhabditis elegans. Dev. Biol. *373*, 184–195.

Kuhn, T.B., Stoeckli, E.T., Condrau, M.A., Rathjen, F.G., and Sonderegger, P. (1991). Neurite outgrowth on immobilized axonin-1 is mediated by a heterophilic interaction with L1(G4). J. Cell Biol. *115*, 1113–1126.

Liu, K.S., and Sternberg, P.W. (1995). Sensory regulation of male mating behavior in Caenorhabditis elegans. Neuron *14*, 79–89.

Lu, Z., Wang, Y., Chen, F., Tong, H., Reddy, M.V., Luo, L., Seshadrinathan, S., Zhang, L., Holthauzen, L.M., Craig, A.M., et al. (2014). Calsyntenin-3 molecular architecture and interaction with neurexin 1α. J. Biol. Chem. *289*, 34530–34542.

Oguro-Ando, A., Zuko, A., Kleijer, K.T., and Burbach, J.P. (2016). A current view on contactin-4, -5, and -6: Implications in neurodevelopmental disorders. Mol. Cell Neurosci. http://dx.doi.org/10.1016/j.mcn.2016.12.004.

Oren-Suissa, M., Bayer, E.A., and Hobert, O. (2016). Sex-specific pruning of neuronal synapses in Caenorhabditis elegans. Nature *533*, 206–211.

Osterhout, J.A., Stafford, B.K., Nguyen, P.L., Yoshihara, Y., and Huberman, A.D. (2015). Contactin-4 mediates axon-target specificity and functional development of the accessory optic system. Neuron *86*, 985–999.

Özkan, E., Carrillo, R.A., Eastman, C.L.,Weiszmann, R.,Waghray, D., Johnson, K.G., Zinn,

582 K., Celniker, S.E., and Garcia, K.C. (2013). An extracellular interactome of
583 immunoglobulin and LRR proteins reveals receptor-ligand networks. Cell *154*, 228–239.
584 Özkan, E., Chia, P.H., Wang, R.R., Goriatcheva, N., Borek, D., Otwinowski, Z., Walz, T.,
585 Shen, K., and Garcia, K.C. (2014). Extracellular architecture of the SYG-1/SYG-2
586 adhesion complex instructs synaptogenesis. Cell *156*, 482–494.
587 Peden, E.M., and Barr, M.M. (2005). The KLP-6 kinesin is required for male mating
588 behaviors and polycystin localization in Caenorhabditis elegans. Curr. Biol. *15*, 394–404.
589 Pettem, K.L., Yokomaku, D., Luo, L., Linhoff, M.W., Prasad, T., Connor, S.A., Siddiqui, T.J.,
590 Kawabe, H., Chen, F., Zhang, L., et al. (2013). The specific α-neurexin interactor
591 calsyntenin-3 promotes excitatory and inhibitory synapse development. Neuron *80*, 113–
592 128.
593 Pocock, R., Bénard, C.Y., Shapiro, L., and Hobert, O. (2008). Functional dissection of the C.
594 elegans cell adhesion molecule SAX-7, a homologue of human L1. Mol. Cell Neurosci. *37*,
595 56–68.
596 Salzberg, Y., Díaz-Balzac, C.A., Ramirez-Suarez, N.J., Attreed, M., Tecle, E., Desbois, M.,
597 Kaprielian, Z., and Bülow, H.E. (2013). Skin-derived cues control arborization of sensory
598 dendrites in Caenorhabditis elegans. Cell *155*, 308–320.
599 Sasakura, H., Inada, H., Kuhara, A., Fusaoka, E., Takemoto, D., Takeuchi, K., and Mori, I.
600 (2005). Maintenance of neuronal positions in organized ganglia by SAX-7, a
601 Caenorhabditis elegans homologue of L1. EMBO J. *24*, 1477–1488.
602 Schwarz, V., Pan, J., Voltmer-Irsch, S., and Hutter, H. (2009). IgCAMs redundantly control
603 axon navigation in Caenorhabditis elegans. Neural Dev. *4*, 13.
604 Serrano-Saiz, E., Oren-Suissa, M., Bayer, E.A., and Hobert, O. (2017). Sexually Dimorphic
605 Differentiation of a C. elegans Hub Neuron Is Cell Autonomously Controlled by a

606 Conserved Transcription Factor. Curr. Biol. *27*, 199–209.

607 Shen, K., and Bargmann, C.I. (2003). The immunoglobulin superfamily protein SYG-1
608 determines the location of specific synapses in C. elegans. Cell *112*, 619–630.

609 Shen, K., Fetter, R.D., and Bargmann, C.I. (2004). Synaptic specificity is generated by the
610 synaptic guidepost protein SYG-2 and its receptor, SYG-1. Cell *116*, 869–881.

611 Shimoda, Y., and Watanabe, K. (2009). Contactins: emerging key roles in the development
612 and function of the nervous system. Cell Adh. Migr. *3*, 64–70.

613 Sperry R.W. (1963). Chemoaffinity in the orderly growth of nerve fiber patterns and
614 connections. Proc. Natl. Acad. Sci. USA *50*, 703–710.

615 Stoeckli, E.T., Sonderegger, P., Pollerberg, G.E., and Landmesser, L.T. (1997). Interference
616 with axonin-1 and NrCAM interactions unmasks a floor-plate activity inhibitory for
617 commissural axons. Neuron *18*, 209–221.

618 Südhof, T.C. (2008). Neuroligins and neurexins link synaptic function to cognitive disease.
619 Nature *455*, 903–911.

620 Uchida, Y., Nakano, S., Gomi, F., and Takahashi, H. (2011). Up-regulation of calsyntenin-3
621 by β-amyloid increases vulnerability of cortical neurons. FEBS Lett. *585*, 651–656.

622 Vagnoni, A., Perkinton, M.S., Gray, E.H., Francis, P.T., Noble, W., and Miller, C.C. (2012).
623 Calsyntenin-1 mediates axonal transport of the amyloid precursor protein and regulates Aβ
624 production. Hum. Mol. Genet. *21*, 2845–2854.

625 White, J.G., Southgate, E., Thomson, J.N., and Brenner, S. (1983). Factors that determine
626 connectivity in the nervous system of Caenorhabditis elegans. Cold Spring Harb. Symp.
627 Quant. Biol. *48*, 633–640.

628 White, J.G. (1985). Neuronal connectivity in Caenorhabditis elegans. Trends Neurosci. *8*,
629 277–283.

White, J.G., Southgate, E., Thomson, J.N., and Brenner, S. (1986). The structure of the nervous system of the nematode Caenorhabditis elegans. Philos. Trans. R Soc. Lond. B Biol. Sci. *314*, 1–340.

Xu, M., Jarrell, T.A., Wang, Y., Cook, S.J., Hall, D.H., and Emmons, S.W. (2013). Computer assisted assembly of connectomes from electron micrographs: application to Caenorhabditis elegans. PLoS One *8*, e54050.

Zallen, J.A., Kirch, S.A., and Bargmann, C.I. (1999). Genes required for axon pathfinding and extension in the C. elegans nerve ring. Development *126*, 3679–3692.

Zhen, M., and Jin, Y. (1999). The liprin protein SYD-2 regulates the differentiation of presynaptic termini in C. elegans. Nature *401*, 371–375.

FIGURE LEGENDS

Figure 1. Cell adhesion protein genes *casy-1* and *rig-6* are required for axon fasciculation. (A) Schematic of the position of cell bodies and axons of three neurons HOA (red), AVG (blue) and a pair of PHC (green) in the male (ventral view). The dashed box indicates the axons and HOA synaptic output analyzed in (C and D) and imaged in (F and H). (B) Electron micrograph showing the axons and synapses of HOA, PHC and AVG. Arrowheads indicate presynaptic density of dyadic synapses of HOA and PHC. Asterisk indicates a mitochondrion. In the schematic, axons are colored as in (A), and presynaptic density is indicated as gray. (C) The number of electron micrograph sections for axon-axon contact between neuron pairs. N2Y series were analyzed from section #13906 to #14249, except for the PHC-AVG (from #13836 to #14249) (WormWiring: http://wormwiring.org). See also Supplementary File 1. (D) Synaptic output of HOA and the connectivity of HOA, AVG and PHC in the boxed region shown in (A). (HOA makes additional connections outside this region.) Synaptic weight determined by electron micrograph section numbers is indicated. The number of sections that contain dyadic synapses (HOA > AVG,PHC or PHC > HOA,AVG) is indicated in parenthesis. (E) Expression of transcriptional reporters for neural cell adhesion genes in the three neurons. One hundred out of 106 neural cell adhesion genes (94%) have been examined and the genes having expression in the three neurons are shown. (F) Distribution of a mCherry-tagged presynaptic marker RAB-3 in HOA axon of wild type or indicated mutants. Arrowheads indicate gaps between the presynaptic puncta. (G) Number of mCherry::RAB-3 puncta in mutants was counted and compared to wild type (n = 30). Error bars are SEM. (H) HOA presynaptic puncta (mCherry::RAB-3; red) were simultaneously visualized with GFP-labeled HOA and AVG axons (green) in wild type, or *casy-1* or *rig-6* mutant animals. Arrowheads indicate the gap region containing smaller or

665 fewer presynaptic puncta. (I) Percentage of axon-axon contact between HOA and AVG in
666 wild type or mutant animals (n = 40). Each dot represents individual animal. Red bar
667 represents the median. (J and K) The mCherry::RAB-3 puncta size (J) or number (K) was
668 measured and compared in the contacting and non-contacting axonal segments between HOA
669 and AVG for the indicated genotypes. The number of the puncta (J) or of axon segments (K)
670 analyzed is indicated below each column. Error bars are SEM.
671 Scale bars, 20 μm. ∗, $P < 0.05$; ∗∗, $P < 0.01$; ∗∗∗, $P < 0.001$ (by Mann-Whitney test).
672
673 **Figure 2. Axon fasciculation defects of *casy-1* and *rig-6* are distinguishable.** (A-D) The
674 axons of the three neurons were individually labeled with wCherry (HOA; red), TagBFP
675 (AVG; blue), and GFP (PHC; green) in wild type (A), *casy-1(tm718)* (B), *rig-6(ok1589)* (C),
676 or *casy-1;rig-6* double mutants (D). Axon fasciculation between each neuronal pair in the
677 dashed box region and schematic of axon fasciculation are shown on the right. Arrowheads
678 indicate the region where two axons are detached from each other. (E) Percentage of axon-
679 axon contact between each neuronal pair in wild type or mutant animals (n = 40). Each dot
680 represents individual animal. Red bar represents the median. (F) Developmental timing of
681 axon extension of the three neurons in males. Each developmental stage was determined by
682 the tail morphology of the male. (G) Axon fasciculation of the three neurons in mock-, PHC-,
683 or HOA-ablated animal. Arrowheads indicate the region where HOA and AVG axons are
684 detached from each other. (H) Percentage of axon-axon contact between each neuronal pair in
685 mock-, PHC-, or HOA-ablated animals. The number of animals analyzed is indicated.
686 Scale bars, 20 μm. ∗, $P < 0.05$; ∗∗, $P < 0.01$; ∗∗∗, $P < 0.001$; ns, not significant (by Mann-
687 Whitney test).
688

689 **Figure 3. CASY-1 and RIG-6 act in postsynaptic AVG for axon fasciculation.** (A and B)
690 Percentage of axon-axon contact between each neuronal pair in animals expressing a full-
691 length *casy-1* (A) or *rig-6* cDNA (B) in postsynaptic AVG or presynaptic HOA or PHC in a
692 respective mutant background (n = 30). The data for wild type and *casy-1* and *rig-6* mutants
693 are identical to those in Figure 2 and are shown for comparison. Each dot represents
694 individual animal. Red bar represents the median. ∗, $P < 0.05$; ∗∗∗, $P < 0.001$; ns, not
695 significant (by Mann-Whitney test). (C and D) Subcellular localization of YFP-tagged
696 CASY-1 (C) or RIG-6 (D) in AVG (green) with the cytoplasmic marker wCherry (red) in L4
697 males. Scale bars, 20 μm.
698 *AVGp*, *inx-18p* (Oren-Suissa et al., 2016); *HOAp*, *eat-4pA* (this study; see Figure 1–figure
699 supplement 1 for expression); *PHCp*, *eat-4p11* (Serrano-Saiz et al., 2017).
700
701 **Figure 4. Structure-function analysis for CASY-1 and RIG-6.** (A and C) Domain structure
702 of mRFP::CASY-1 and its deletion constructs (A) or of YFP::RIG-6 and its deletion
703 constructs (C) with the summary of rescue activity when expressed in AVG of *casy-1* or *rig-6*
704 mutant animals. SP, signal peptide; Cad, cadherin domain; LNS, laminin neurexin sex
705 hormone binding protein domain; TM, transmembrane; Intra, intracellular domain; Ig,
706 immunoglobulin domain; FN[III], fibronectin type III domain. (B and D) Percentage of axon-
707 axon contact between each neuronal pair in animals expressing the indicated deletion
708 constructs for CASY-1 (B) or RIG-6 (D) in AVG of *casy-1* or *rig-6* mutant animals (n = 30).
709 Note that Full-Ct (CASY-1::YFP) in (B) and Full (YFP::RIG-6) in (D) were the same
710 transgenes used for protein localization in Figure 3, and rescued axon fasciculation defects in
711 mutants. The data for wild type and *casy-1* and *rig-6* mutants are the same as shown in Figure
712 2. Each dot represents individual animal. Red bar represents the median. ∗, $P < 0.05$; ∗∗, $P <$

713 0.01; ***, $P < 0.001$; ns, not significant (by Mann-Whitney test).

714

715 **Figure 5. BAM-2 interacts with CASY-1.** (A) Distribution of a mCherry-tagged presynaptic
716 marker RAB-3 in HOA axon of wild type or *bam-2(cy6)* mutants. Arrowheads indicate gaps
717 between the presynaptic puncta. (B) Number of mCherry::RAB-3 puncta in *bam-2* mutants
718 was counted and compared to wild type (n = 30). Error bars are SEM. (C) Images of axon
719 placement of HOA, AVG and PHC in *bam-2* and *casy-1;bam-2* double mutants. Axon
720 fasciculation between each neuronal pair in the dashed box region and schematic of axon
721 fasciculation are shown on the right. Arrowheads indicate the region where two axons are
722 detached from each other. (D) Percentage of axon-axon contact between each neuronal pair in
723 wild type or mutant animals (n = 40). Each dot represents individual animal. Red bar
724 represents the median. (E) Percentage of axon-axon contact between each neuronal pair in
725 animals expressing a full-length *bam-2* cDNA in HOA or PHC in *bam-2* mutant background
726 (n = 30). In (C-E), the data for wild type and *casy-1* mutants are the same as shown in Figure
727 2. (F) Co-immunoprecipitation of CASY-1 and BAM-2.
728 Scale bars, 20 μm. **, $P < 0.01$; ***, $P < 0.001$; ns, not significant (by Mann-Whitney test).

729

730 **Figure 6. SAX-7 interacts with RIG-6.** (A) Distribution of a mCherry-tagged presynaptic
731 marker RAB-3 in HOA axon of wild type or *sax-7(nj48)* mutants. Arrowheads indicate gaps
732 between the presynaptic puncta. (B) Number of mCherry::RAB-3 puncta in *sax-7* mutants
733 was counted and compared to wild type (n = 30). Error bars are SEM. (C) Images of axon
734 placement of HOA, AVG and PHC in *sax-7* and *rig-6;sax-7* double mutants. Axon
735 fasciculation between each neuronal pair in the dashed box region and schematic of axon
736 fasciculation are shown on the right. Arrowheads indicate the region where two axons are

detached from each other. (D) Percentage of axon-axon contact between each neuronal pair in wild type or mutant animals (n = 40). Each dot represents individual animal. Red bar represents the median. (E) Percentage of axon-axon contact between each neuronal pair in animals expressing the short isoform *sax-7s* or long isoform *sax-7l* cDNA in HOA or PHC in *sax-7* mutant background (n = 30). In (C-E), the data for wild type and *rig-6* mutants are the same as shown in Figure 2. (F) Co-immunoprecipitation of RIG-6 and SAX-7S. (G) Images of axon placement of HOA and AVG in PHC-ablated animals expressing *sax-7s* cDNA in HOA (*Ex[HOAp::sax-7s]*). Arrowheads indicate the region where the HOA axon is detached from the AVG axon. (H) Percentage of axon-axon contact between HOA and AVG in PHC-ablated animals either expressing or not expressing *sax-7s* cDNA in HOA. The number of animals analyzed is indicated. The data for PHC-ablated wild type animals are the same as shown in Figure 2H.

Scale bars, 20 μm. *, $P < 0.05$; **, $P < 0.01$; ***, $P < 0.001$; ns, not significant (by Mann-Whitney test).

Figure 7. Cell adhesion genes required for male mating behavior. Vulva location efficiency (A) or response efficiency (B) in the indicated mutant males was measured and compared to wild type males. The number of males analyzed is indicated below each column. Error bars are SEM. ***, $P < 0.001$ (by Mann-Whitney test).

Figure 8. Model for function of cell adhesion protein interactions. (A) Three pathways additively act to achieve the wild type level of HOA-AVG axon fasciculation. The median percentages of HOA-AVG axon fasciculation in mutant and/or PHC ablation studies were used to estimate contribution of each pathway. (B) Schematic showing axons, cell adhesion

761 protein interactions, and their putative function during the L4-adult transition in males. In L4
762 stage, the PHC axon contacts the AVG axon through RIG-6-SAX-7S interaction. In adult
763 stage, close apposition of HOA and AVG membranes involves CASY-1-BAM-2 interaction,
764 while unidentified protein interaction may mediate contact between HOA and PHC. These
765 protein interactions regulate the probability of axon fasciculation and vulva location behavior
766 possibly by controlling synapse formation between the neurons.
767

768 **SUPPLEMENTARY FILES**

769 **Supplementary File 1. Neighborhood and synapse in the HOA-AVG-PHC circuit.**

770 **Supplementary File 2. *C. elegans* strains, molecular cloning and transgenes**

771

Figure 1

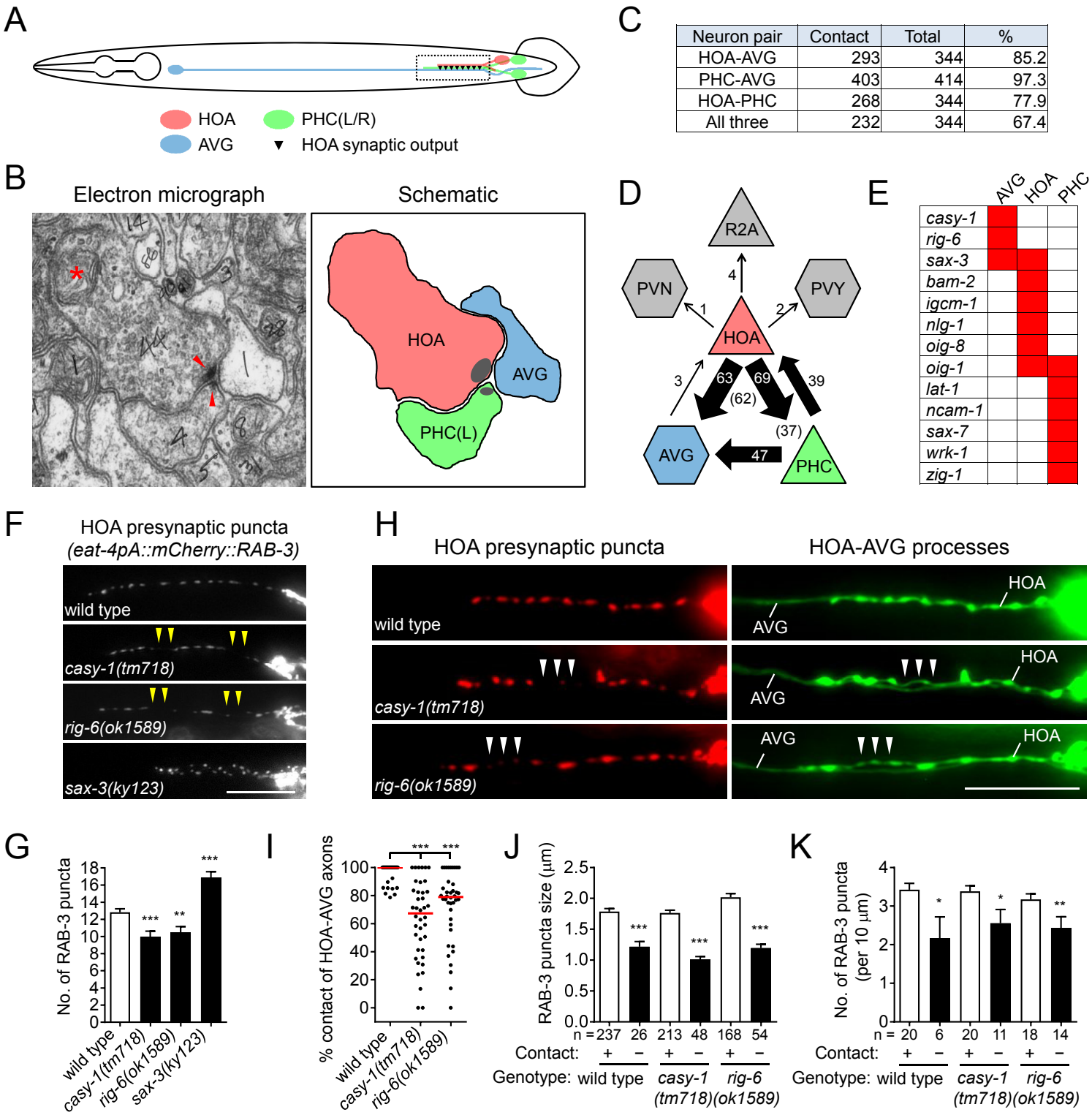

Figure 2

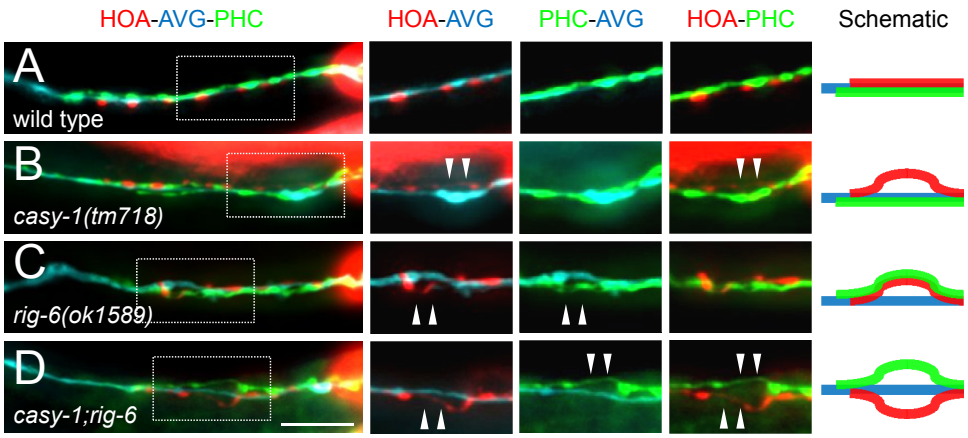

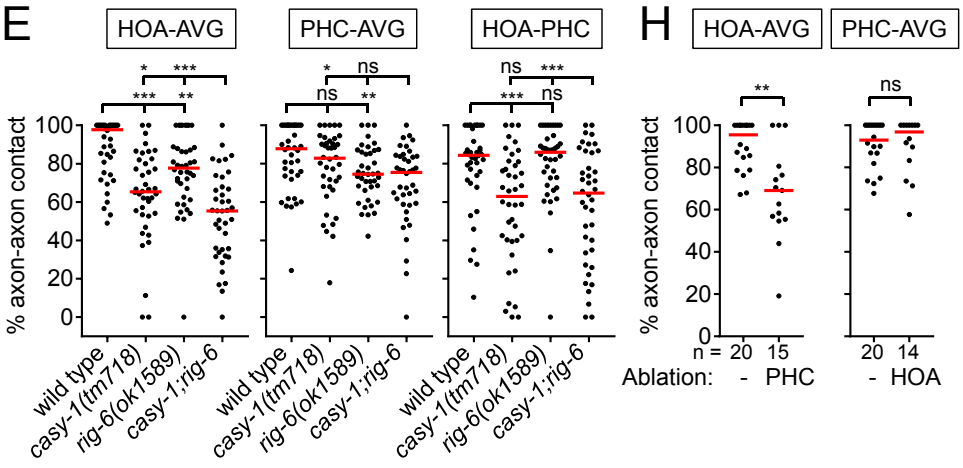

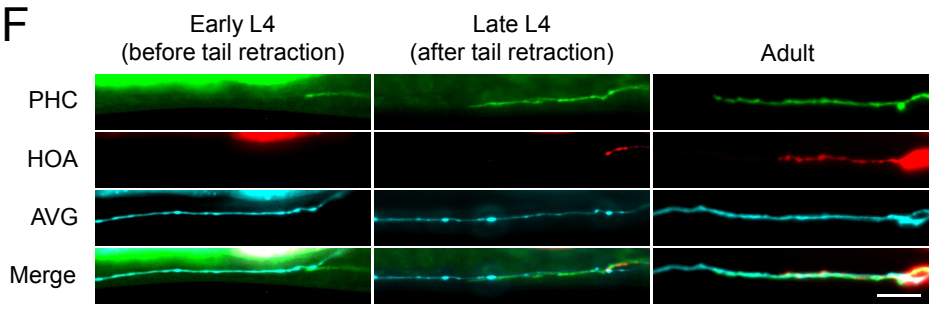

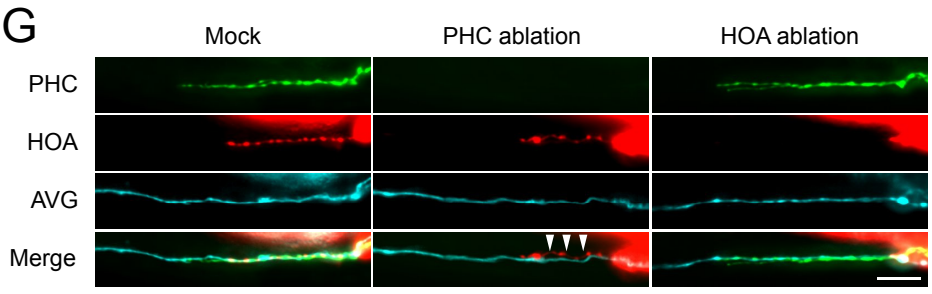

Figure 3

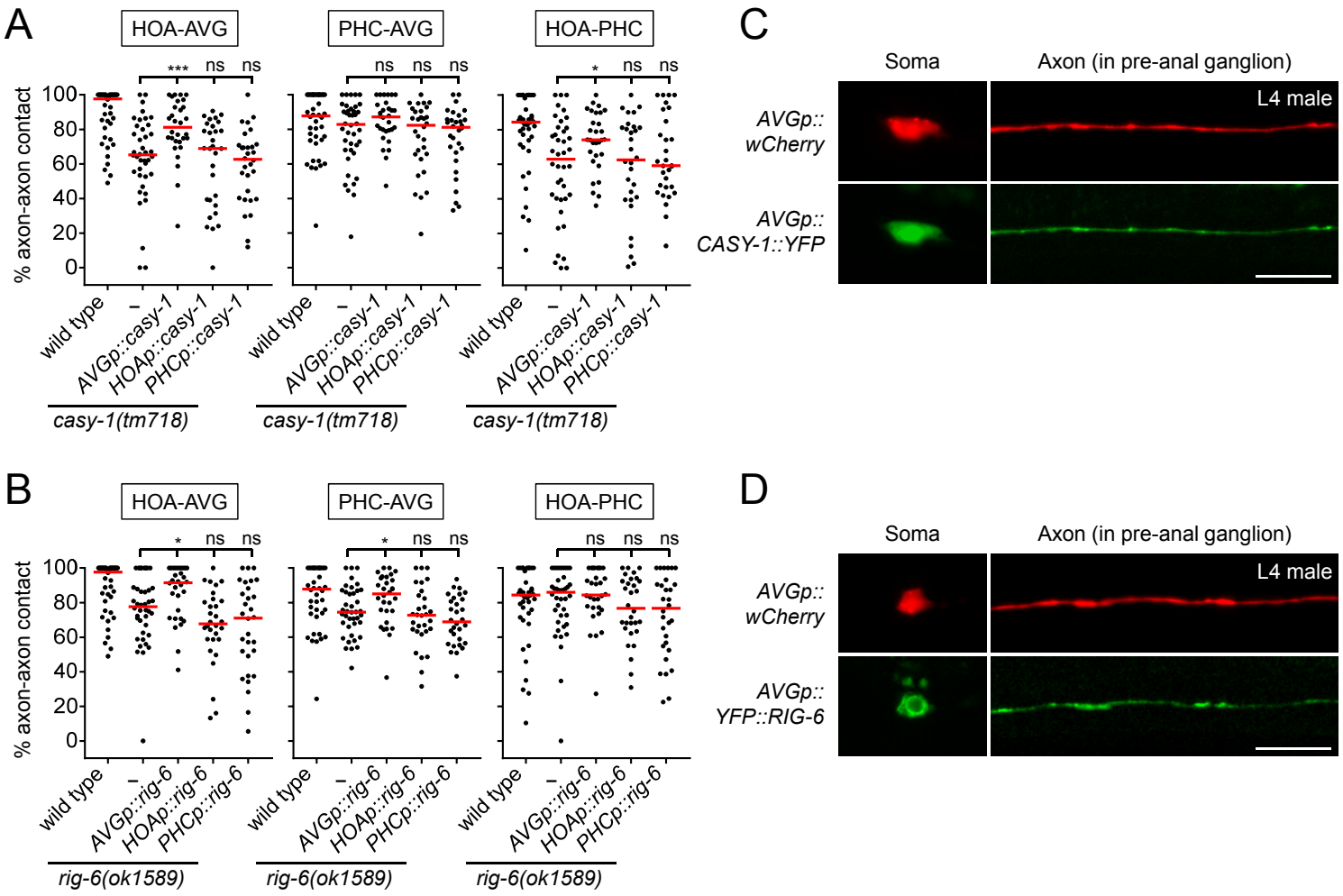

Figure 4

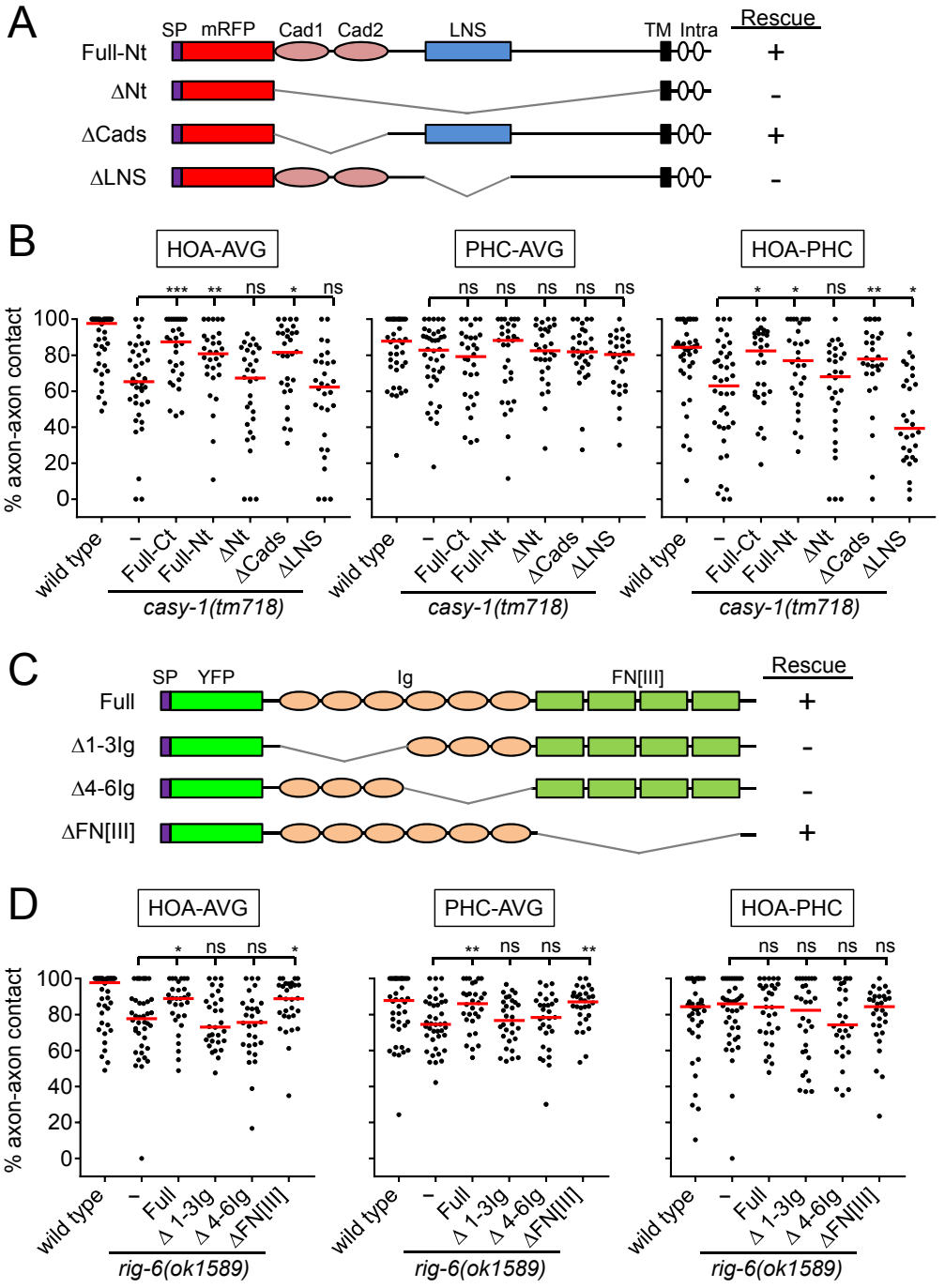

Figure 5

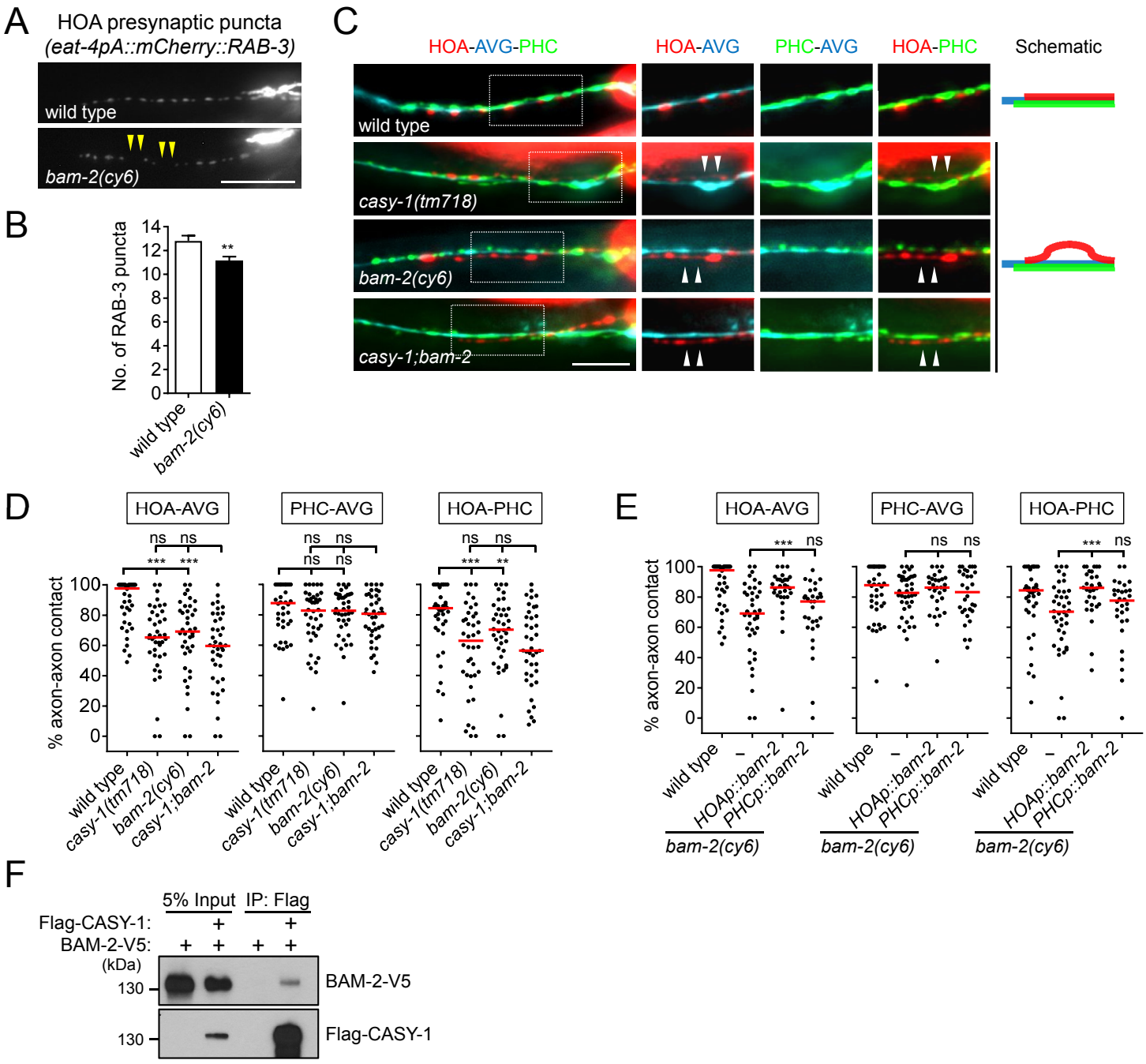

Figure 6

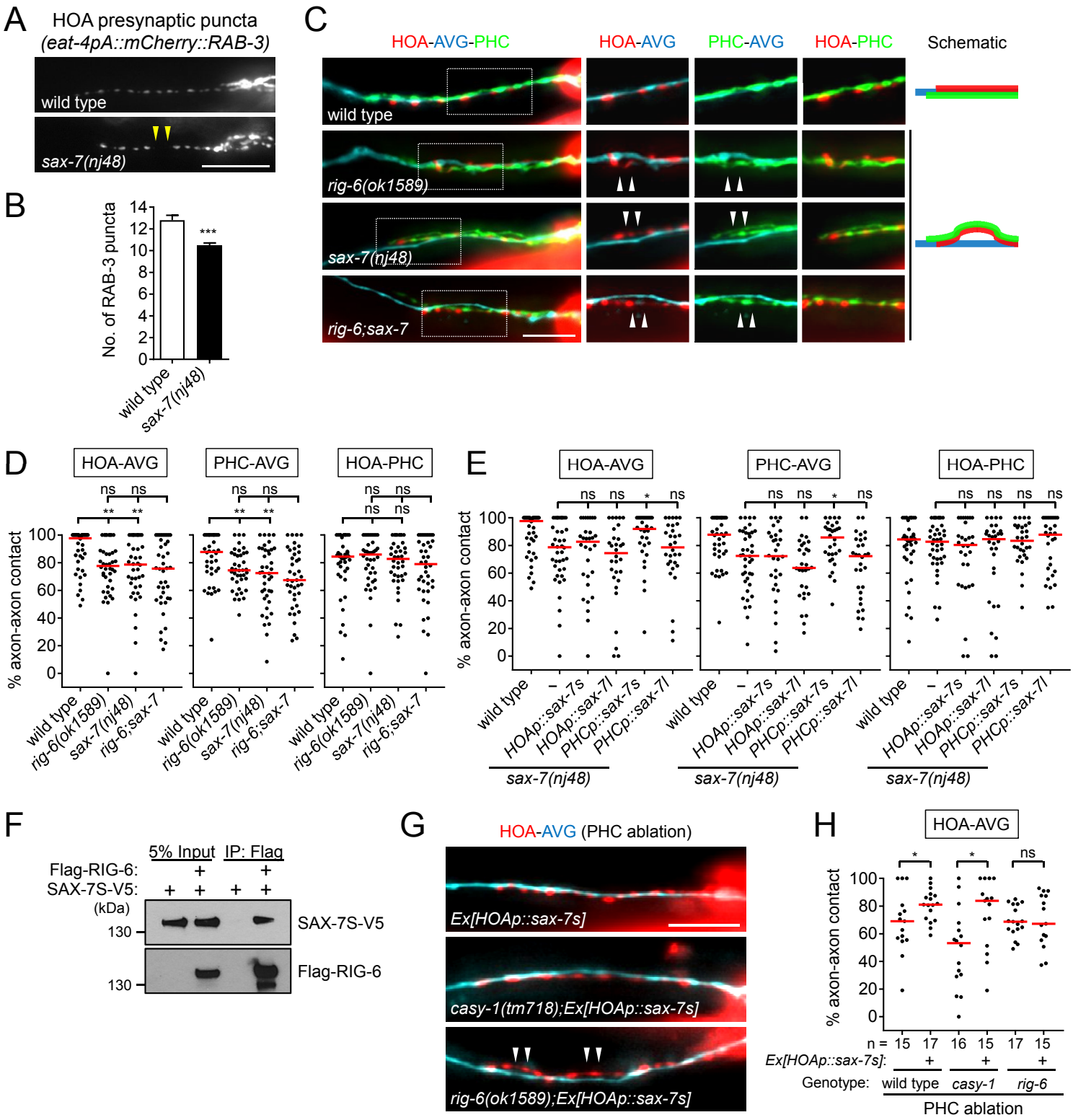

Figure 7

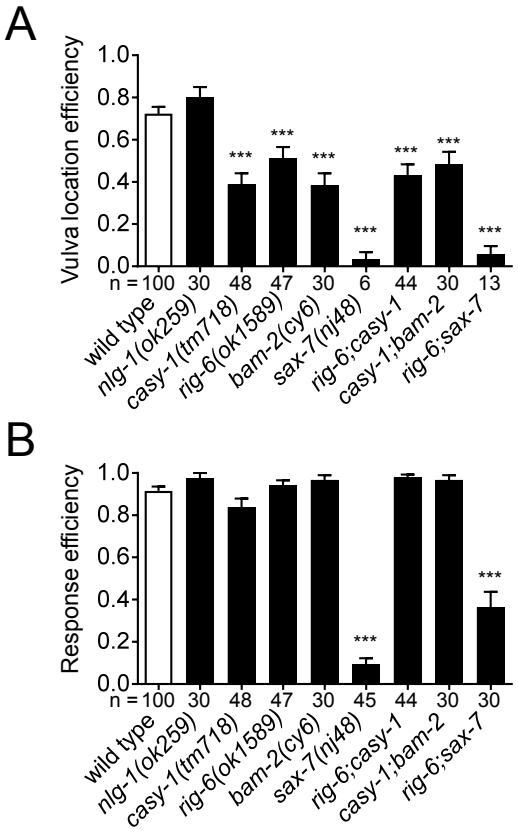

Figure 8

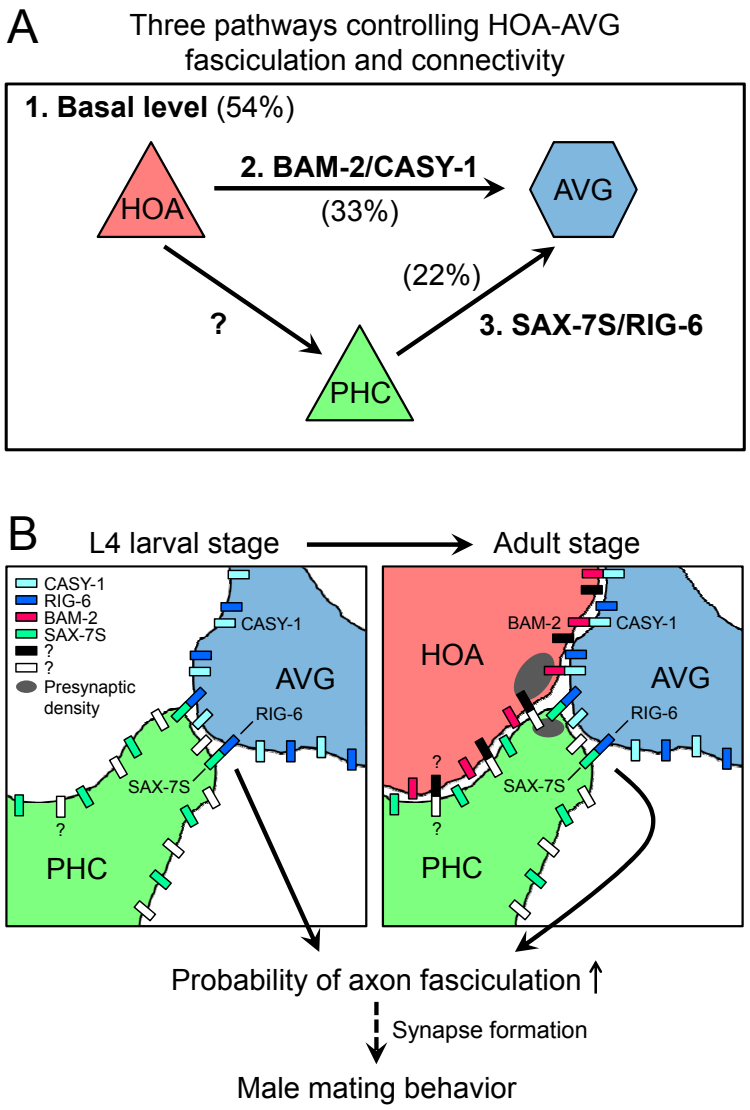

Figure 1—figure supplement 1

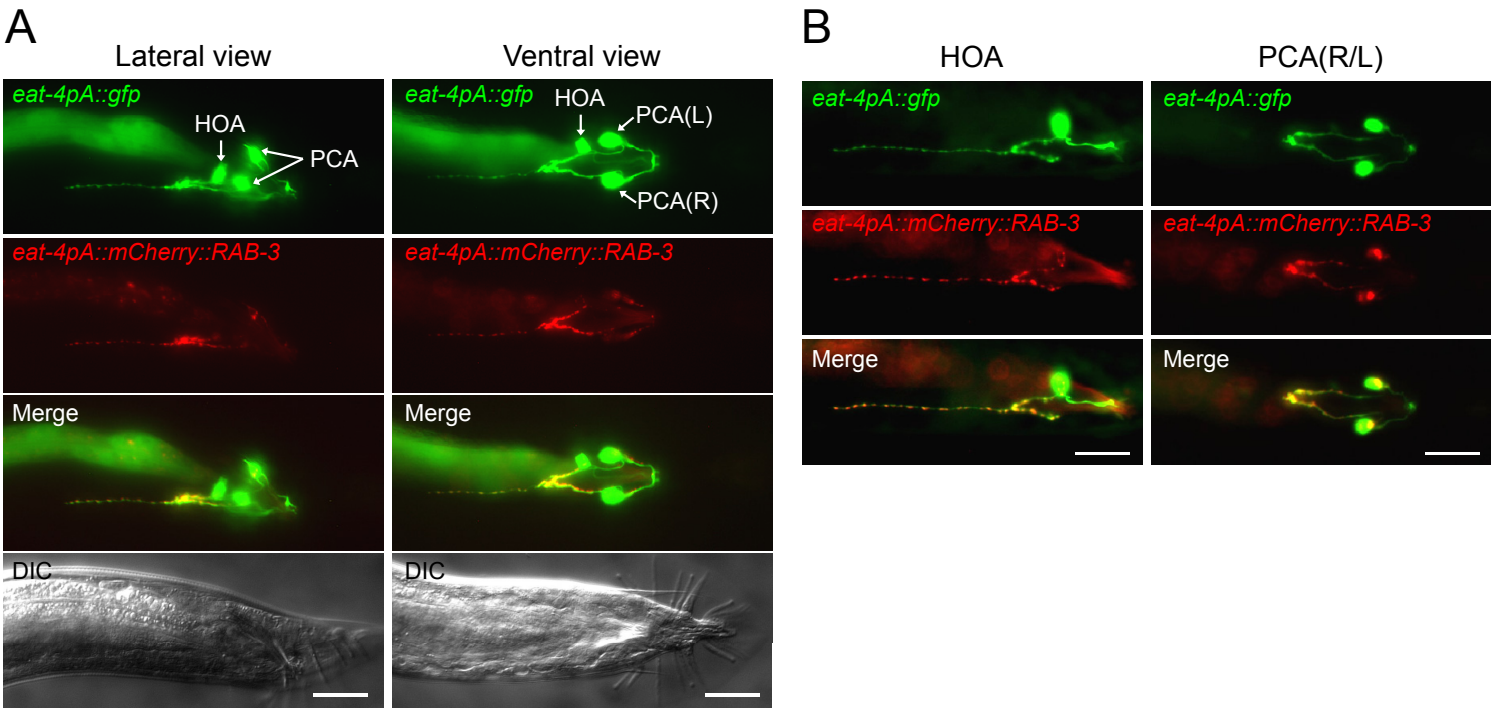

Figure 1—figure supplement 1. Visualizing HOA presynapses.
(A) Lateral and ventral views of the tail region of animals carrying *eat-4pA::gfp* (green) and *eat-4pA::mcherry::RAB-3* (red). The *eat-4pA* is a fragment of *eat-4* promoter and drives expression only in HOA and PCA in the male tail.
(B) Images of mosaic expression in HOA or PCA in transgenic animals used in (A). HOA, but not PCA, has an anteriorly-oriented projection with discrete RAB-3 puncta.
Scale bars, 20 μm.

Figure 1—figure supplement 2

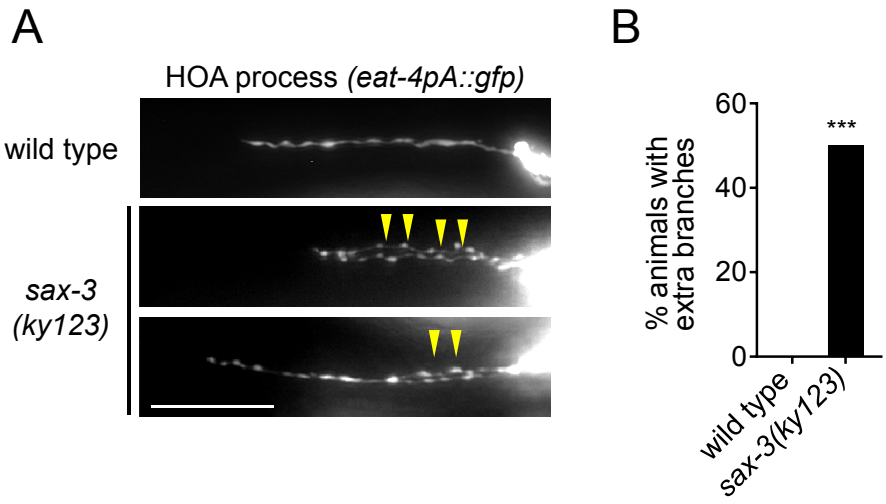

Figure 1—figure supplement 2. Extra branching of HOA in *sax-3(ky123)* mutants.
(A) HOA axon of wild type or *sax-3(ky123)* mutants. Arrowheads indicate extra branches of HOA. Scale bar, 20 μm.
(B) Percentage of animals with extra branches of HOA was measured and compared to wild type (n = 50). ***, $P < 0.001$ (by Fisher's exact test).

Figure 1—figure supplement 3

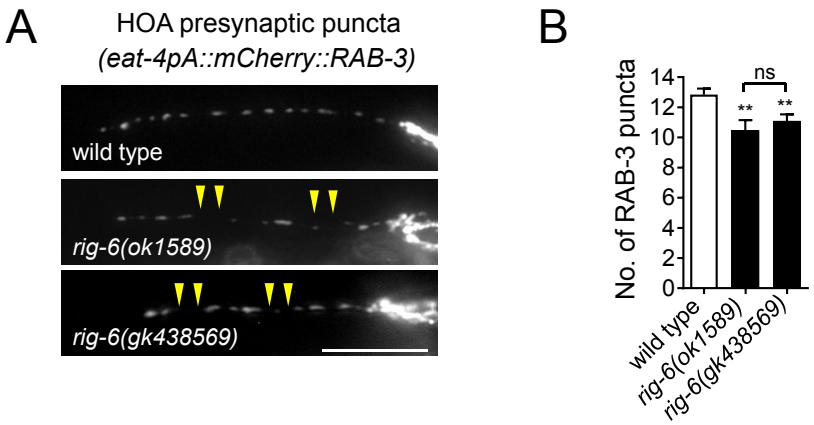

Figure 1—figure supplement 3. Phenotypes of *rig-6(gk438569)* mutants.
(A) Distribution of a mCherry-tagged presynaptic marker RAB-3 in HOA axon of *rig-6(gk438569)* mutants. Arrowheads indicate gaps between the presynaptic puncta. Scale bar, 20 μm.
(B) Number of mCherry::RAB-3 puncta in mutants was counted and compared to wild type (n = 30). Error bars are SEM.
The data for wild type and *rig-6(ok1589)* mutants are identical to those in Figure 1 and are shown for comparison. **, $P < 0.01$; ns, not significant (by Mann-Whitney test).

Figure 2—figure supplement 1

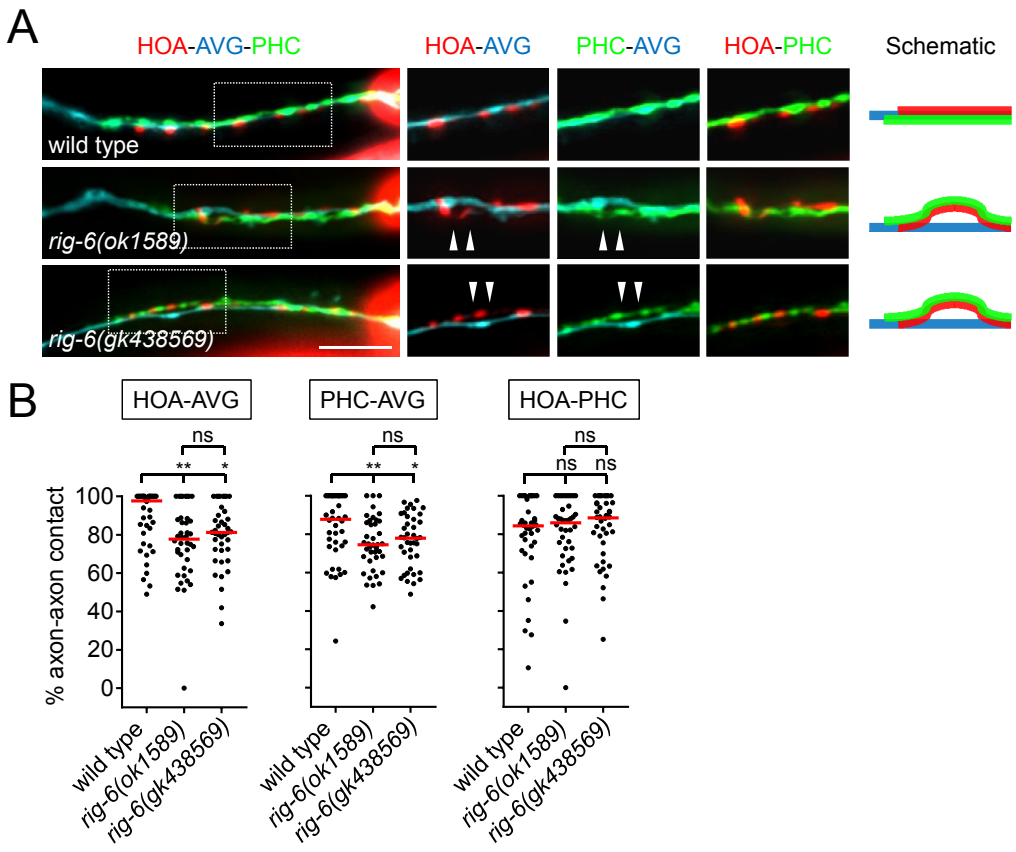

Figure 2—figure supplement 1. Phenotypes of *rig-6(gk438569)* mutants.
(A) Images of axon placement of HOA, AVG and PHC in *rig-6(gk438569)* mutants. Axon fasciculation between each neuronal pair in the dashed box region and schematic of axon fasciculation are shown on the right. Arrowheads indicate the region where two axons are detached from each other. Scale bar, 20 μm.
(B) Percentage of axon-axon contact between each neuronal pair in *rig-6(gk438569)* mutant animals (n = 40). Each dot represents individual animal. Red bar represents the median.
The data for wild type and *rig-6(ok1589)* mutants are identical to those in Figure 2 and are shown for comparison. *, $P < 0.05$; **, $P < 0.01$; ns, not significant (by Mann-Whitney test).

Figure 3—figure supplement 1

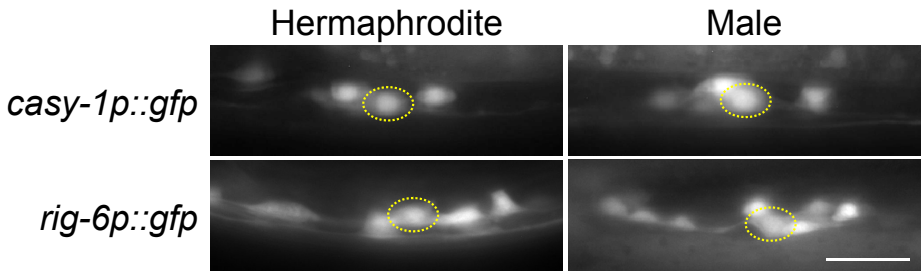

Figure 3—figure supplement 1. *casy-1* and *rig-6* are expressed in AVG in both sexes. Transcriptional reporter lines carrying *casy-1p::gfp* and *rig-6p::gfp* were examined for expression in AVG in adult hermaphrodites or males. Location of AVG cell body was identified by Nomarski optics and is indicated as dashed circle. Scale bar, 20 μm.

Figure 5—figure supplement 1

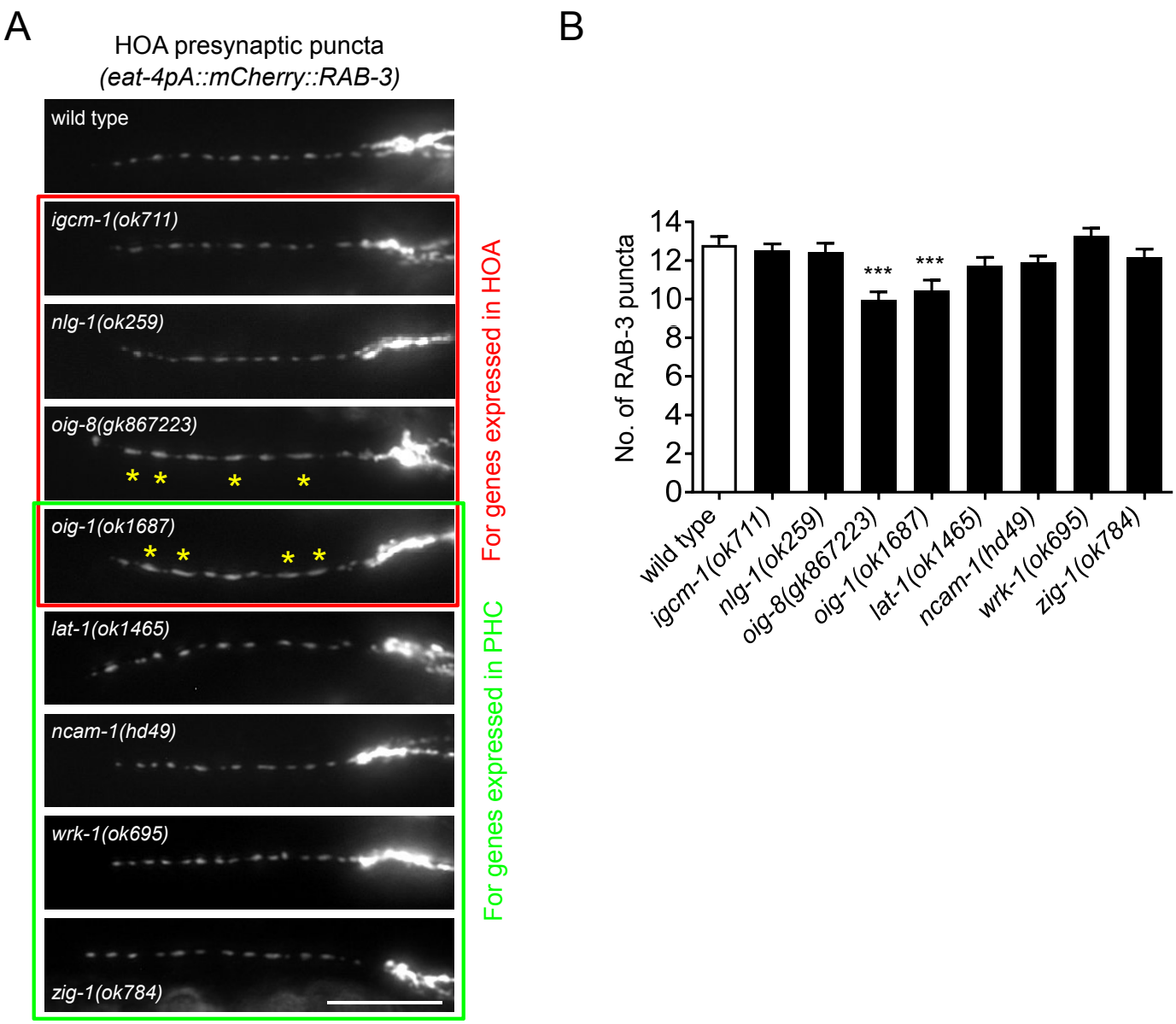

Figure 5—figure supplement 1. HOA presynaptic puncta phenotypes of mutants for cell adhesion genes.

(A) Distribution of a mCherry-tagged presynaptic marker RAB-3 in HOA axon of mutants for cell adhesion genes expressed in HOA (red box) or PHC (green box). Expression pattern of these genes is shown in Figure 1E. Asterisks indicate diffused puncta. Scale bar, 20 μm

(B) Number of mCherry::RAB-3 puncta in mutants was counted and compared to wild type (n = 30). Error bars are SEM. ***, $P < 0.001$ (by Mann-Whitney test). In *oig-1* and *oig-8* mutants, the puncta numbers were decreased due to the diffused puncta, of which cause is still elusive. The data for wild type are the same as shown in Figure 5.

Figure 5—figure supplement 2

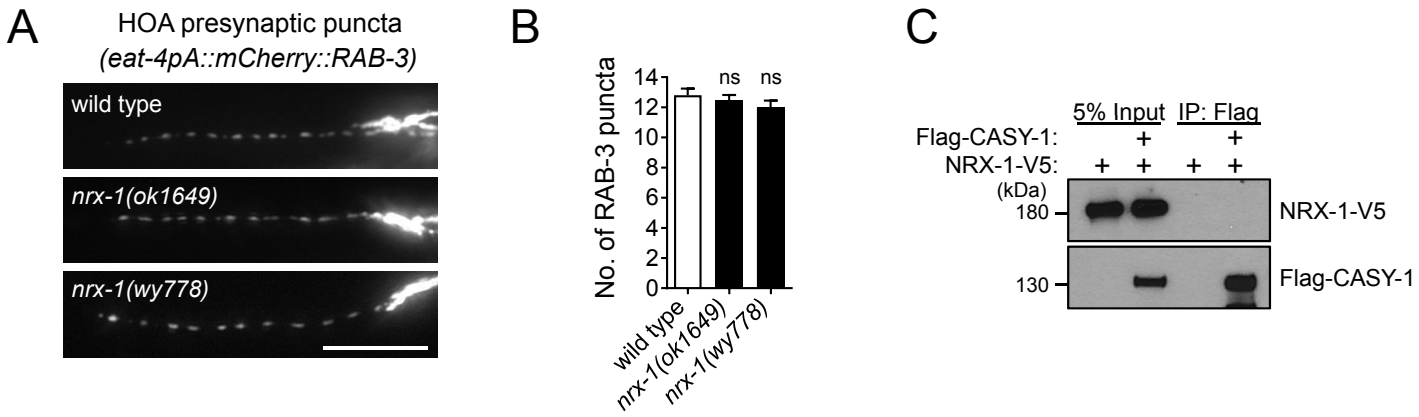

Figure 5—figure supplement 2. NRX-1 does not interact with CASY-1.
(A) Distribution of a mCherry-tagged presynaptic marker RAB-3 in HOA axon of a hypomorphic *nrx-1(ok1649)* and a null *nrx-1(wy778)* mutants. Scale bar, 20 μm
(B) Number of mCherry::RAB-3 puncta in mutants was counted and compared to wild type (n = 30). Error bars are SEM. ns, not significant (by Mann-Whitney test).
(C) Co-immunoprecipitation assay for CASY-1 and NRX-1.
The data for wild type are the same as shown in Figure 5.

Supplementary File 2. *C. elegans* strains, molecular cloning and transgenes

Fluorescent reporter strains for cell adhesion gene expression

Strain name	Transgene	Strain background	Reporter for
EM1162	*sEx10331[rCesB0034.3a::GFP + pCeh361]*[1]	*dpy-5(e907) I; him-5(e1490) V*	*casy-1*
EM1176	*sEx12431[rCesC09E7.3::GFP + pCeh361]*[1]	*dpy-5(e907) I; him-5(e1490) V*	*oig-1*
EM1191	*sIs10411[rCes B0457.1::GFP + pCeh361]*[1]	*dpy-5(e907) I; him-5(e1490) V*	*lat-1*
EM1168	*sIs13247[rCesC40C9.5::GFP + pCeh361]*[1]	*dpy-5(e907) I; him-5(e1490) V*	*nlg-1*
EM1195	*hdEx333[rig-6a::YFP + pha-1(+)]*[2]	*pha-1(e2123) III; him-5(e1490) V*	*rig-6*
EM1199	*hdEx335[ncam-1a::YFP + pha-1(+)]*[2]	*pha-1(e2123) III; him-5(e1490) V*	*ncam-1*
EM1200	*hdEx341[igcm-1::YFP + pha-1(+)]*[2]	*pha-1(e2123) III; him-5(e1490) V*	*igcm-1*
EM1188	*otIs25[zig-1::GFP + pRF4(rol-6)]*[3]	*him-5(e1490) V*	*zig-1*
EM1205	*bxEx170[oig-8p::GFP + pRF4(rol-6)]*[4]	*him-5(e1490) V*	*oig-8*
EM1278	*bxEx228[sax-3p::YFP + pRF4(rol-6)]*[4]	*him-5(e1490) V*	*sax-3*
EM1254	*bxEx204[bam-2p::YFP + pCeh361]*[4]	*dpy-5(e907) I; him-5(e1490) V*	*bam-2*
EM1282	*bxEx232[wrk-1p::YFP + pCeh361]*[4]	*dpy-5(e907) I; him-5(e1490) V*	*wrk-1*
EM1294	*bxEx244[sax-7p::YFP + pCeh361]*[4]	*dpy-5(e907) I; him-5(e1490) V*	*sax-7*

[1]Original transgene was previously described (Hunt-Newbury et al., 2007).
[2]Original transgene was previously described (Schwarz et al., 2009).
[3]Original transgene was previously described (Aurelio et al., 2002).
[4]Transgene generated in this study

Molecular cloning and constructs

eat-4pA::gfp, *eat-4pA::wCherry*, and *eat-4pA::mCherry::RAB-3*

eat-4pA, a 419 bp promoter fragment of the *eat-4* gene (-5457 ~ -5039 bp), was PCR-amplified from *pPC52* (a gift from L. García) with restriction sites of SphI and XmaI. This PCR product was digested and ligated into SphI/XmaI-digested *pPD95.75* vector to generate *eat-4pA::gfp*, into SphI/XmaI-digested *inx-18p::wCherry* (Oren-Suissa et al., 2016) to generate *eat-4pA::wCherry*, or into SphI/XmaI-digested *pkd-2p::mCherry::RAB-3* (a gift from M. Lázaro-Peña) to generate *eat-4pA::mCherry::RAB-3*. *eat-4pA* drives expression in the male-specific sensory neurons HOA and PCAs.

inx-18p::gfp, *inx-18p::wCherry*, and *inx-18p::TagBFP*

inx-18p::wCherry was described previously (Oren-Suissa et al., 2016). To generate *inx-18p::gfp*, *inx-18p* fragment was digested with SphI and XmaI from *inx-18p::wCherry* and cloned into SphI/XmaI-digested *pPD95.75* vector. *inx-18p::TagBFP* was obtained by a PCR-fusion method (Hobert, 2002). *inx-18p* was PCR-amplified from *inx-18p::wCherry* and then fused to *TagBFP* amplified from *myo-3p::TagBFP* (a gift from H. Bülow) to generate *inx-18p::TagBFP* PCR fragment. *inx-18p* drives expression in the sex-shared interneuron AVG (occasionally in URX) (Oren-Suissa et al., 2016).

eat-4p11::gfp

eat-4p11::gfp was described previously (Serrano-Saiz et al., 2017). *eat-4p11* is highly expressed in the sex-shared sensory/interneuron PHC in males but hardly detectable in hermaphrodites (Serrano-Saiz et al., 2017).

casy-1 constructs for rescue experiment

To generate *inx-18p::casy-1* and *eat-4pA::casy-1*, *casy-1* cDNA was PCR-amplified from *casy-1p::casy-1* (Ikeda et al., 2008) with restriction sites of KpnI and NaeI, and then digested and ligated into the KpnI/NaeI sites of *inx-18p::wCherry* and *eat-4pA::wCherry*, respectively. To generate *eat-4p11::casy-1*, the promoter region of *inx-18p::casy-1* was replaced by *eat-4p11* using restriction sites of SphI and XmaI.

To generate *inx-18p::casy-1::yfp*, *casy-1* cDNA was PCR-amplified from *casy-1p::casy-1* and then fused to *yfp* amplified from *pPD136.64* vector. This PCR fusion product was digested and ligated into the KpnI/NaeI sites of *inx-18p::wCherry* to replace *wCherry* with *casy-1::yfp*.

casy-1 deletion constructs with *ins-1* promoter were described previously (Ikeda et al., 2008). To generate *inx-18p::mRFP::casy-1*(Full-Nt), *inx-18p::mRFP::casy-1-ΔNt* (ΔNt), *inx-18p::mRFP::casy-1-ΔCads* (ΔCads), and *inx-18p::mRFP::casy-1-ΔLNS* (ΔLNS), each of *mRFP*-tagged *casy-1* fragments was PCR-amplified from the *ins-1p* driven constructs with restriction sites of KpnI and NaeI. These PCR products were digested and ligated into the KpnI/NaeI sites of *inx-18p::wCherry* to replace *wCherry* with the *mRFP*-tagged *casy-1* fragments.

rig-6 constructs for rescue experiment

rig-6 cDNA that encodes a long isoform RIG-6d was obtained from total RNA of worms using iScript cDNA synthesis Kit (Bio-Rad) by two rounds of PCR reactions (primer F: 5′-ACTACAACGATGATGATGCTT-3′ and primer R: 5′-ACTGGGATGAAAGAATTGGGAAC-3′ for the first round; primer F: 5′-GGGGGGTACCATGATGATGCTTATTCGGTGTATT-3′ and primer R: 5′-GGGGTTTAAACTTAGAGTCTCCATAGTAATAATAA-3′ for the second round). The PCR product was digested with KpnI and PmeI and ligated into the KpnI/NaeI sites of *inx-18p::wCherry* to generate *inx-18p::rig-6*. The *rig-6* cDNA sequence was verified by sequencing.

To generate *eat-4pA::rig-6* and *eat-4p11::rig-6*, *eat-4pA* and *eat-4p11* fragments derived from *eat-4pA::wCherry* and *eat-4p11::gfp* with SphI/KpnI digestion were ligated into the SphI/KpnI sites of *inx-18p::rig-6* to replace *inx-18p*.

To generate *inx-18p::yfp::rig-6*, the *rig-6* signal sequence plus *yfp* was PCR-amplified from *pPD136.64* vector and fused to the remaining sequence of *rig-6* cDNA amplified from *inx-18p::rig-6* (primer F: 5′-CCCCGGTACCATGATGATGCTTATTCGGTGTATT-3′ and primer R: 5′-GGGGAGGCCTTTAGAGTCTCCATAGTAATAATAA-3′). This PCR fusion product was digested with KpnI and StuI and ligated into the KpnI/NaeI sites of *inx-18p::wCherry* to replace *wCherry* with *yfp::rig-6*.

rig-6 deletion constructs including *inx-18p::yfp::rig-6-Δ1-3Ig* (Δ1-3Ig), *inx-18p::yfp::rig-6-Δ4-6Ig* (Δ4-6Ig), and *inx-18p::yfp::rig-6-ΔFnIII* (ΔFnIII), were generated by mutagenesis of *inx-18p::yfp::rig-6* (Full) using Q5 Site-Directed Mutagenesis Kit (New England Biolabs). The sequence was verified by sequencing. The full-length of *rig-6* cDNA is 3591 bp and deleted regions for the constructs are: 430 ~ 1320 bp for Δ1-3Ig, 1321 ~ 2199 bp for Δ4-6Ig, and 2200 ~ 3504 bp for ΔFnIII.

bam-2 constructs for rescue experiment

bam-2 cDNA was obtained from the *yk2037j22* clone (a gift from Y. Kohara). The sequence was verified by sequencing. To generate *eat-4pA::bam-2* and *eat-4p11:: bam-2*, a full-length *bam-2* cDNA was PCR-amplified from the *yk2037j22* clone with restriction sites of KpnI and NaeI, and then digested and ligated into the KpnI/NaeI sites of *eat-4pA::wCherry* and *eat-4p11::casy-1*, respectively.

sax-7 constructs for rescue experiment

ttx-3p::sax-7s and *ttx-3p::sax-7l* were described previously (Díaz-Balzac et al., 2015). To generate *eat-4pA::sax-7s* and *eat-4pA::sax-7l*, *eat-4pA* fragment derived from *eat-4pA::casy-1* with HindIII/KpnI digestion was ligated into the HindIII/KpnI sites of *ttx-3p::sax-7s* and *ttx-3p::sax-7l* to replace *ttx-3p*. To generate *eat-4p11::sax-7s* and *eat-4p11::sax-7l*, *eat-4p11* fragment derived from *eat-4p11::gfp* with HindIII/KpnI digestion was ligated into the HindIII/KpnI sites of *ttx-3p::sax-7s* and *ttx-3p::sax-7l* to replace *ttx-3p*.

Constructs for mammalian cell expression

To generate *pCMV8::3xFLAG::casy-1*, *casy-1* cDNA was PCR-amplified without the start (ATG) and signal sequence with restriction sites of NotI and XmaI, and then digested and ligated into the NotI/XmaI sites of *pCMV8::3xFLAG::egl-15A* (Díaz-Balzac et al., 2015) to replace *egl-15A* with *casy-1*.

To generate *pCMV8::3xFLAG::rig-6*, *rig-6* cDNA was PCR-amplified without the start (ATG) and signal sequence with restriction sites of NotI and StuI, and then digested and ligated into the NotI/SmaI sites of *pCMV8::3xFLAG::egl-15A* to replace *egl-15A* with *rig-6*.

pcDNA3.1::sax-7s::V5 was described previously (Díaz-Balzac et al., 2015). To generate *pcDNA3.1::bam-2::V5*, *bam-2* cDNA was amplified without the stop codon with restriction sites of KpnI and ApaI, and then digested and ligated into the KpnI/ApaI sites of *pcDNA3.1::sax-7s::V5* to replace *sax-7s* with *bam-2*.

To generate *pcDNA3.1::nrx-1::V5*, *nrx-1* cDNA was amplified from *gcy-8p::BirA::nrx-1* (Desbois et al., 2015) without the stop codon with restriction sites of KpnI and ApaI, and then digested and ligated into the KpnI/ApaI sites of *pcDNA3.1::sax-7s::V5* to replace *sax-7s* with *nrx-1*.

Transgenic strains

Strain name	Transgene name	DNA on array	Strain background
Reporter strains			
EM1322	*bxEx263*	*eat-4pA::gfp 25ng/µl, eat-4pA::mCherry::RAB-3 10ng/µl*	*him-5(e1490) V*
EM1330	*bxIs25*	*eat-4pA::gfp 25ng/µl, eat-4pA::mCherry::RAB-3 10ng/µl*	*him-5(e1490) V*
EM1404	*bxEx298*	*eat-4pA::gfp 25ng/µl, inx-18p::gfp 25ng/µl, eat-4pA::mCherry::RAB-3 25ng/µl*	*him-5(e1490) V*
EM1462	*bxIs29*	*eat-4p11::gfp 50ng/µl, eat-4pA::wcherry 25ng/µl, inx-18p::TagBFP 25ng/µl*	*him-5(e1490) V*
Strains for protein localization			
EM1463	*bxEx312*	*inx-18p::casy-1::yfp 5ng/µl, inx-18p::wCherry 25ng/µl, ttx-3::gfp 50ng/µl*	*him-5(e1490) V*
EM1536	*bxEx334*	*inx-18p::yfp::rig-6 25ng/µl, inx-18p::wCherry 25ng/µl, ceh-22p::gfp 50ng/µl*	*him-5(e1490) V*
Strains for rescue experiments			
EM1505	*bxEx287*	*inx-18p::casy-1 25ng/µl, ttx-3::mCherry 25ng/µl*	*casy-1(tm718) II; him-5(e1490) V*
	bxIs29	see above	
EM1506	*bxEx285*	*eat-4pA::casy-1 25ng/µl, ttx-3::mCherry 25ng/µl*	*casy-1(tm718) II; him-5(e1490) V*
	bxIs29	see above	
EM1507	*bxEx304*	*eat-4p11::casy-1 25ng/µl, ttx-3::gfp 50ng/µl*	*casy-1(tm718) II; him-5(e1490) V*
	bxIs29	see above	
EM1514	*bxEx312*	see above	*casy-1(tm718) II; him-5(e1490) V*
	bxIs29	see above	
EM1513	*bxEx289*	*inx-18p::mRFP::casy-1 5ng/µl, ceh-22::gfp 25ng/µl*	*casy-1(tm718) II; him-5(e1490) V*
	bxIs29	see above	
EM1520	*bxEx292*	*inx-18p::mRFP::casy-1-ΔNt 5ng/µl, ceh-22::gfp 25ng/µl*	*casy-1(tm718) II; him-5(e1490) V*
	bxIs29	see above	
EM1508	*bxEx294*	*inx-18p::mRFP::casy-1-ΔCads 5ng/µl, ceh-22::gfp 25ng/µl*	*casy-1(tm718) II; him-5(e1490) V*
	bxIs29	see above	
EM1509	*bxEx296*	*inx-18p::mRFP::casy-1-ΔLNS 5ng/µl, ceh-22::gfp 25ng/µl*	*casy-1(tm718) II; him-5(e1490) V*
	bxIs29	see above	
EM1491	*bxEx306*	*inx-18p::rig-6 5ng/µl, ttx-3::gfp 50ng/µl*	*rig-6(ok1589) II; him-5(e1490) V*
	bxIs29	see above	
EM1492	*bxEx308*	*eat-4pA::rig-6 5ng/µl, ttx-3::gfp 50ng/µl*	*rig-6(ok1589) II; him-5(e1490) V*
	bxIs29	see above	
EM1493	*bxEx310*	*eat-4p11::rig-6 5ng/µl, ttx-3::gfp 50ng/µl*	*rig-6(ok1589) II; him-5(e1490) V*
	bxIs29	see above	
EM1527	*bxEx334*	see above	*rig-6(ok1589) II; him-5(e1490) V*
	bxIs29	see above	
EM1543	*bxEx340*	*inx-18p::yfp::rig-6-Δ1-3Ig 5ng/µl, ttx-3::gfp 50ng/µl*	*rig-6(ok1589) II; him-5(e1490) V*
	bxIs29	see above	
EM1545	*bxEx342*	*inx-18p::yfp::rig-6-Δ4-6Ig 5ng/µl, ttx-3::gfp 50ng/µl*	*rig-6(ok1589) II; him-5(e1490) V*
	bxIs29	see above	

EM1547	*bxEx344*	*inx-18p::yfp::rig-6-ΔFnIII 5ng/µl, ttx-3::gfp 50ng/µl*	*rig-6(ok1589) II; him-5(e1490) V*
	bxIs29	see above	
EM1539	*bxEx336*	*eat-4pA::bam-2 5ng/µl, ttx-3::gfp 50ng/µl*	*bam-2(cy6) I; him-5(e1490) V*
	bxIs29	see above	
EM1541	*bxEx338*	*eat-4p11::bam-2 5ng/µl, ttx-3::gfp 50ng/µl*	*bam-2(cy6) I; him-5(e1490) V*
	bxIs29	see above	
EM1496	*bxEx322*	*eat-4pA::sax-7l 5ng/µl, ttx-3::gfp 50ng/µl*	*sax-7(nj48) IV; him-5(e1490) V*
	bxIs29	see above	
EM1498	*bxEx324*	*eat-4pA::sax-7s 5ng/µl, ttx-3::gfp 50ng/µl*	*sax-7(nj48) IV; him-5(e1490) V*
	bxIs29	see above	
EM1500	*bxEx326*	*eat-4p11::sax-7l 5ng/µl, ttx-3::gfp 50ng/µl*	*sax-7(nj48) IV; him-5(e1490) V*
	bxIs29	see above	
EM1502	*bxEx328*	*eat-4p11::sax-7s 5ng/µl, ttx-3::gfp 50ng/µl*	*sax-7(nj48) IV; him-5(e1490) V*
	bxIs29	see above	
EM1535	*bxEx324*	see above	*him-5(e1490) V*
	bxIs29	see above	
EM1549	*bxEx324*	see above	*casy-1(tm718) II; him-5(e1490) V*
	bxIs29	see above	
EM1550	*bxEx324*	see above	*rig-6(ok1589) II; him-5(e1490) V*
	bxIs29	see above	
Mutant strains with reporters			
EM1414	*bxEx298*	see above	*casy-1(tm718) II; him-5(e1490) V*
EM1425	*bxEx298*	see above	*rig-6(ok1589) II; him-5(e1490) V*
EM1333	*bxIs25*	see above	*oig-1(ok1687) III; him-5(e1490) V*
EM1334	*bxIs25*	see above	*nlg-1(ok259) X; him-5(e1490) V*
EM1344	*bxIs25*	see above	*zig-1(ok784) II; him-5(e1490) V*
EM1346	*bxIs25*	see above	*casy-1(tm718) II; him-5(e1490) V*
EM1347	*bxIs25*	see above	*rig-6(ok1589) II; him-5(e1490) V*
EM1348	*bxIs25*	see above	*igcm-1(ok711) X; him-5(e1490) V*
EM1349	*bxIs25*	see above	*oig-8(gk867223) II ;him-5(e1490) V*
EM1368	*bxIs25*	see above	*nrx-1(ok1649) him-5(e1490) V*
EM1412	*bxIs25*	see above	*ncam-1(hd49) X; him-5(e1490) V*
EM1416	*bxIs25*	see above	*lat-1(ok1465)/mIn1 II; him-5(e1490) V*
EM1436	*bxIs25*	see above	*wrk-1(ok695) X; him-5(e1490) V*
EM1459	*bxIs25*	see above	*sax-7(nj48) IV; him-5(e1490) V*

EM1489	*bxIs25*	see above	*nrx-1(wy778) him-5(e1490) V*
EM1511	*bxIs25*	see above	*sax-3(ky123) X; him-5(e1490) V*
EM1531	*bxIs25*	see above	*rig-6(gk438569) II; him-5(e1490) V*
EM1533	*bxIs25*	see above	*bam-2(cy6) I; him-5(e1490) V*
EM1477	*bxIs29*	see above	*rig-6(ok1589) II; him-5(e1490) V*
EM1481	*bxIs29*	see above	*rig-6(ok1589) casy-1(tm718) II; him-5(e1490) V*
EM1482	*bxIs29*	see above	*casy-1(tm718) II; him-5(e1490) V*
EM1483	*bxIs29*	see above	*sax-7(nj48) IV; him-5(e1490) V*
EM1521	*bxIs29*	see above	*rig-6(ok1589) II; sax-7(nj48) IV; him-5(e1490) V*
EM1522	*bxIs29*	see above	*bam-2(cy6) I; him-5(e1490) V*
EM1530	*bxIs29*	see above	*rig-6(gk438569) II; him-5(e1490)V*
EM1537	*bxIs29*	see above	*bam-2(cy6) I; casy-1(tm718) II; him-5(e1490) V*

Strains for mating behavior

Mutant strains were crossed at least twice into *him-5(e1490) V*. These include: *casy-1(tm718) II; him-5(e1490) V*, *rig-6(ok1589) II; him-5(e1490) V*, *bam-2(cy6) I; him-5(e1490) V*, *sax-7(nj48) IV; him-5(e1490) V*, *nlg-1(ok259) X; him-5(e1490) V*, *casy-1(tm718) rig-6(ok1589) II; him-5(e1490) V*, *casy-1(tm718) II; bam-2(cy6) I; him-5(e1490) V*, *rig-6(ok1589) II; sax-7(nj48) IV; him-5(e1490) V*.